NACA TN No. 1521

NATIONAL ADVISORY COMMITTEE FOR AERONAUTICS

TECHNICAL NOTE

No. 1521

FULL-SCALE INVESTIGATION OF THE BLADE MOTION OF THE PV-2 HELICOPTER ROTOR

By Eugene Migotsky

Langley Memorial Aeronautical Laboratory
Langley Field, Va.

FOR REFERENCE

NOT TO BE TAKEN FROM THIS ROOM

Washington
March 1948

LIBRARY COPY

JUN 2 0 1981

LANGLEY RESEARCH CENTER
LIBRARY, NASA
HAMPTON, VIRGINIA

3 1176 01434 0476

NATIONAL ADVISORY COMMITTEE FOR AERONAUTICS

TECHNICAL NOTE NO. 1521

FULL-SCALE INVESTIGATION OF THE BLADE MOTION OF THE PV-2 HELICOPTER ROTOR

By Eugene Migotsky

SUMMARY

An experimental investigation of the PV-2 helicopter rotor has been conducted at the Langley Laboratory of the National Advisory Committee for Aeronautics to determine the basic performance characteristics of a fully articulated rotor. Results are presented of the blade-motion observations at the 0.75-radius station for a limited range of flight conditions. The flapping and feathering motions of the rotor blade have been presented as the variation of the harmonic coefficients of these motions with mean pitch angle and tip-speed ratio for a series of rotor shaft-angle settings. The results have also been summarized in a convenient set of charts from which the flapping and the feathering motions of such a rotor may be obtained rapidly for the range of conditions covered in these tests. In addition, the data have been compared with the blade motions predicted from theoretical studies.

For the range of these tests the magnitude of the measured flapping motion is small (less than 1°) when the rotor is trimmed about a point on the shaft approximately 1/3 radius below the flapping hinge. The second harmonics of the flapping motion are very small, less than 0.25°. Both the lateral and longitudinal components of the feathering increase in magnitude with tip-speed ratio and thrust coefficient. Within the range of these tests, relatively large errors that were found to occur in determining the resultant force vector appear to give only secondary errors in the determination of the blade-motion coefficients (useful drag-lift ratio $(D/L)_u$ between 0.04 and 0.2).

The method of calculating blade motions presented in NACA Report No. 716 is based on the assumption of uniform inflow across the rotor disk. This method was found to predict the coning angle and the longitudinal component of the equivalent flapping to an accuracy of about 0.5°. This method gave values of the lateral component of equivalent flapping about 1° to 1.5° smaller than the experimental values, although the trends of the calculated curves plotted against tip-speed ratio and thrust coefficient were similar. The use of an inflow that increases linearly from the front to the rear of the rotor, as calculated in NACA ARR No. L5E10, accounts for about one-half the difference between the data and the uniform inflow calculations.

INTRODUCTION

An experimental investigation of the PV-2 helicopter rotor has been conducted at the Langley full-scale tunnel to determine the basic performance characteristics of a fully articulated rotor. The investigation was intended to provide large-scale data which would be used to determine the validity of existing theory and which would aid in making rational evaluations of proposed helicopter designs.

In addition to measurements of the rotor forces and power input to the rotor, photographic observations of the blade motions were made during these tests. Static-thrust and forward-flight data were obtained, the latter being measured at tip-speed ratios ranging from approximately 0.1 to 0.2. Inasmuch as vibrational difficulties were encountered at the design rotor speed, it was necessary to conduct the tests at reduced rotational speeds and the tests were, in effect, about two-thirds of full scale.

The results of the static-thrust and forward-flight force-test data, together with a comparison with theoretical predictions, have been presented in reference 1. The present paper contains the results of the forward-flight blade-motion observations.

The blade-flapping and blade-feathering motions are given for the 0.75-radius station. For a few high-tip-speed-ratio conditions, the blade twist was also checked. The results are presented as the variation of the harmonic coefficients of the blade motions with tip-speed ratio, mean pitch angle, and rotor shaft-angle setting. This presentation of the blade-motion data is essentially the same as that of the force-test data in reference 1. In addition, the blade-motion coefficients are presented as functions of thrust coefficient and useful drag-lift ratio.

A comparison is made between these data and the theoretical blade motions calculated by the method of reference 2, which assumes a uniform inflow over the rotor disk. In addition, the data are compared with theoretical calculations based on the nonuniform inflow of reference 3.

SYMBOLS

R	rotor-blade radius, feet
r	blade-element radius, feet
b	number of blades
c	blade chord of untapered part, feet

σ rotor solidity $\left(\frac{bc}{\pi R}\right)$

Ω angular velocity, radians per second

V forward velocity, feet per second

μ tip-speed ratio $\left(\frac{V \cos \alpha}{\Omega R} \text{ with } \cos \alpha \text{ assumed equal to } 1.0\right)$

λ ratio of axial-flow velocity to rotor-blade tip speed

ρ air density, slugs per cubic foot

I_1 mass moment of inertia of rotor blade about flapping hinge, slug-feet^2

a slope of curve of lift coefficient against angle of attack of blade airfoil section, radian measure

γ mass constant of one rotor blade $\left(\frac{c\rho a R^4}{I_1}\right)$

B tip-loss factor (blade elements outboard of BR are assumed to have drag but no lift)

T rotor thrust, pounds

C_T thrust coefficient $\left(\frac{T}{\rho(\Omega R)^2 \pi R^2}\right)$

L rotor lift, pounds

$(D/L)_u$ useful drag-lift ratio, ratio of rotor resultant force along flight path to rotor lift

f equivalent flat-plate drag area, square feet $\left(\frac{\text{Parasite drag}}{\frac{1}{2}\rho V^2}\right)$

ψ blade azimuth angle measured from downwind position in direction of rotation, degrees

M_w weight moment of blade about flapping hinge, pound-feet

β equivalent blade flapping angle; measured from plane perpendicular to zero-feathering axis, degrees; approximated by following expression:

$$\beta = a_0 - a_1 \cos \psi - b_1 \sin \psi - a_2 \cos 2\psi - b_2 \sin 2\psi$$

β_s measured blade flapping angle; measured from plane perpendicular to shaft axis, degrees; approximated by following expression:

$$\beta_s = a_{0_s} - a_{1_s} \cos \psi - b_{1_s} \sin \psi - a_{2_s} \cos 2\psi - b_{2_s} \sin 2\psi$$

θ_s measured pitch angle of zero-lift line; measured from plane perpendicular to shaft axis, degrees; approximated by following expression for feathering motion:

$$\theta_s = A_{0_s} + A_{1_s} \cos \psi + B_{1_s} \sin \psi$$

α angle of attack of zero-feathering axis, acute angle between direction of air flow and plane perpendicular to zero-feathering axis, negative when inclined forward, degrees

α_s angle of attack of shaft axis, acute angle between direction of air flow and plane perpendicular to shaft axis, negative when inclined forward, degrees

α_{s_T} rotor shaft-angle setting; angle of attack of rotor shaft uncorrected for jet-boundary effect, degrees

a_0 constant term in Fourier series that expresses β (radians); hence, the rotor coning angle

a_n coefficient of $\cos n\psi$ in expression for β

b_n coefficient of $\sin n\psi$ in expression for β

APPARATUS AND TESTS

The PV-2 rotor tested was 25 feet in diameter and had three blades constructed of wood and fabric. The blades were of NACA 0012.6 section, were not twisted, and had no taper except for cut-outs at the inboard end. Pertinent characteristics of the blades are given in figure 1. The mass characteristics of the blades were determined by weighing and swinging the blades. The rotor was designed to operate at a thrust coefficient of 0.00364 (gross weight of 1000 lb at 371 rpm).

The PV-2 rotor had hinges which permitted the blades to oscillate in the plane of rotation (dragging) as well as normal to the plane of rotation (flapping). Variation of blade pitch angle was obtained by means of a

movable-bearing mechanism; moving the bearing parallel to the shaft changed the mean pitch angle of the blades, and tilting the bearing with respect to the shaft provided cyclic variation of pitch angle with azimuth angle. The rotor was provided with hydraulic dampers which helped to damp the blade dragging motion. In addition, rubber restrainers were used to restrict elastically the blade flapping and blade dragging motions. These restrainers were relatively soft; for example, when a blade was at its maximum flapping angle, the bending moment imposed on the spar was numerically equal to the static-weight moment of the blade. Furthermore, the flapping restrainers were adjusted to exert no force on the blades in normal hovering flight.

A photograph of the PV-2 helicopter rotor mounted in the Langley full-scale tunnel is shown in figure 2. The rotor hub was located approximately on the center line of the jet and about 20 feet from the entrance cone. A description of the support system, balances, and instrumentation relating to the measurement of forces and power is given in reference 1.

A photographic system was used to record the blade motions. Grain-of-wheat bulbs were installed at the 0.45-radius, 0.75-radius, and 0.95-radius stations on the leading and trailing edges of one of the blades. A motor-driven 35-millimeter motion-picture camera, mounted on the rotor hub and rotating with it, recorded the blade motions. A photograph of this setup is shown in figure 3. The camera on the rotor hub also photographed lights located on the test chamber wall at known azimuth angles; namely, the 260°, 270°, and the 280° azimuth positions for the rotor-shaft axis perpendicular to the tunnel axis. The use of three sets of lights at 10° intervals assured that at least one set would be photographed during each revolution for the field of view of the lens, the camera speed, and the rotor speeds used in these tests. The azimuth angles for frames which did not photograph the wall lights (about 8 or 9 frames per revolution) were found by assuming that the rotor speed and camera speed were constant during the revolution. It is believed that, with this system of recording the blade motions, the azimuth angles were determined within ±5°, the flapping angles within ±0.15°, and the pitch angles within ±0.30°.

The tests were conducted under conditions corresponding to trim (zero moment) about a representative center-of-gravity location, which in this case was taken to be on the shaft axis and $47\frac{5}{8}$ inches below the flapping hinge. All records of the blade motions were taken simultaneously with the force-test data. The measurements were made at several rotor speeds, tip-speed ratios, and rotor-shaft-angle settings.

As a result of vibration difficulties (described in reference 1) the maximum rotor speed for the data presented in this paper is 280 rpm. The data obtained at the reduced rotor speeds correspond, in effect, to those of a rotor tested at about two-thirds of full scale. The lowest

tip-speed ratio, determined by the minimum value of steady air-stream velocity in the wind tunnel, was about 0.11 for the rotor speeds attainable; the maximum value was about 0.23.

RESULTS AND DISCUSSION

Measured Results

The flapping and pitch angles measured with respect to a plane perpendicular to the shaft axis were first plotted against azimuth angle for each test condition. Figure 4 shows a typical plot of this form for one value of tip-speed ratio, rotor shaft-angle setting, and mean pitch angle. The harmonic coefficients of these curves were obtained by means of 12-point harmonic analyses and the variations of these coefficients with mean pitch angle, tip-speed ratio, and rotor-shaft-angle setting are presented. Only the motion of the 0.75-radius station is given. The blade twist was checked for a few of the higher tip-speed ratio conditions but, within the accuracy of the pitch-angle measurements, no twist was found and the motion of the 0.75-radius station is considered to be typical of the entire blade.

In addition to the measured blade motions, the coefficients of the equivalent flapping measured with respect to the plane perpendicular to the zero feathering axis are presented. Locke (reference 4) showed, by referring the blade motion to the plane of the blade tips, that the flapping rotor with no cyclic pitch is identical to a feathering or nonflapping rotor, having the axis of rotation inclined at an angle a_1 to the shaft axis of the flapping rotor. This analysis can be extended to rotors which have various combinations of flapping and feathering and such rotors can be regarded as either equivalent nonfeathering or nonflapping rotors. Inasmuch as existing rotor theory has been developed in general for a nonfeathering rotor, it is convenient to view the rotor tested as such by converting the feathering into flapping and by considering the equivalent flapping motion measured with respect to the plane perpendicular to the zero feathering axis. For the rotor in which the feathering is a simple harmonic function of azimuth angle and the blade motions about the shaft axis are approximated by the expressions listed in the symbols, the conversion formulas are as follows:

$$a_1 = a_{1_s} - B_{1_s}$$

$$b_1 = b_{1_s} + A_{1_s}$$

$$\alpha = \alpha_s + B_{1_s}$$

The coning angle a_{0_s} and the second harmonics of the flapping angles a_{2_s} and b_{2_s} remain unchanged.

The presentation of the blade-motion coefficients follows essentially along the same lines as that of the force-test parameters in reference 1. The coefficients of the equivalent flapping as well as the measured blade motion were first plotted against the mean pitch angle for different tip-speed ratios at fixed rotor shaft-angle settings. Figures 5 to 7 show these coefficients plotted in this manner for a sample rotor shaft-angle setting of -5.5° and give an indication of the scatter in the data. Although the second harmonics of the feathering were computed from the 12-point harmonic analyses, their magnitudes were less than the accuracy and, consequently, they have been omitted.

From the plots of the blade-motion coefficients against A_0, cross plots were made to obtain the variation of these coefficients with μ for fixed values of A_0 and α_{s_T}; these variations are presented in figure 8 for the sample rotor-shaft-angle setting of -5.5°. The second harmonics of the measured flapping motions are independent of tip-speed ratio and of rotor shaft-angle setting within the accuracy of these tests and, consequently, were not cross-plotted.

In figures 9 to 11 the parameters A_0 and α_{s_T} have been replaced with the more significant parameters $(D/L)_u$ and C_T. The blade-motion coefficients in these charts have been plotted against $(D/L)_u$ for thrust coefficients of 0.00268, 0.00364, and 0.00446 which, in the case of the PV-2 rotor, correspond to disk loadings of 1.50, 2.04, and 2.50, respectively, and are given for five values of μ ranging from 0.12 to 0.20. With the charts of figures 9 to 11 the blade motion of a rotor can be estimated directly for the range of conditions represented in the charts if only C_T and $(D/L)_u$ are known.

These charts, which show the blade-motion coefficients as functions of $(D/L)_u$, were obtained by determining the values of A_0 and $(D/L)_u$ corresponding to each combination of C_T, μ, and α_{s_T} from figure 13 of reference 1. The values of the blade-motion coefficients corresponding to these values of A_0 were then obtained from charts similar to those of figure 8, which cover the range of shaft angles for the desired values of C_T, μ, and α_{s_T}, and the blade-motion coefficients were plotted against $(D/L)_u$. Because of the scatter in the data and the limited number of rotor-shaft-angle settings at which data were available, straight lines were faired through all the values thus obtained.

These charts show that relatively large errors in determining $(D/L)_u$ will result in only secondary errors in the determination of the flapping and feathering coefficients within the range of these tests ($(D/L)_u$ between 0.04 and 0.2).

For direct application to the PV-2 helicopter, a further set of curves is presented in figure 12 in which $(D/L)_u$ has been assumed to correspond at every point to level unaccelerated flight of a helicopter having an equivalent flat-plate area f of 7 square feet (the value assumed in reference 1). The variations of the measured blade-motion coefficients with tip-speed ratio are shown in this figure for the three values of thrust coefficient chosen. The variations with tip-speed ratio of the equivalent flapping coefficients are given in figure 13 for the same thrust coefficients. For $C_T = 0.00446$ the coefficients were obtained by extrapolating the curves to very small positive values of $(D/L)_u$. The variations of the first harmonics of the flapping and feathering motions with thrust coefficient are given in figures 14 and 15 for two values of tip-speed ratio.

Figures 12 to 15 show that the measured flapping is small, less than 1°, for the rotor that is feathered to trim about a point below the rotor head and on the axis of rotation. The lateral flapping b_{1_s} is very small and increases with C_T, but is practically independent of μ; the longitudinal flapping a_{1_s} increases almost linearly with μ and is essentially independent of C_T. The coning angle a_{0_s} varies only slightly with μ, but increases with C_T since the ratio of blade thrust to blade centrifugal force increases. The second harmonics of the flapping motion, in all cases, are very small, being less than 0.25°.

Both components of feathering, or cyclic pitch, required to trim the rotor about a typical center-of-gravity location increase in magnitude with μ and C_T. Consequently, in order to change the forward speed of a machine equipped with this rotor and operating at constant thrust coefficient and rotor speed, lateral as well as longitudinal control must be applied.

Comparison with Theory

Also included in figures 12 to 15 are the theoretical flapping coefficients as calculated by the method of reference 2 for a nonfeathering rotor having the following characteristics:

$$\sigma = 0.0605$$

$$a = 5.56 \text{ per radian}$$

$$\gamma = 10.16$$

$$M_W = 95.8 \text{ pound-feet}$$

$$I_1 = 25.14 \text{ slug-feet}^2$$

$$\Omega = 28.25 \text{ radians per second}$$

$$B = 0.97$$

The theoretical and experimental second harmonics, as shown in figure 12, are small and the agreement is reasonable. Whereas the predicted value of a_{2_s} is slightly lower than the experimental value obtained in these tests, the difference is within the accuracy with which the feathering coefficients could be determined and the second harmonics of feathering would be expected to modify the second harmonic flapping.

The coning angle a_0 and the longitudinal component of the flapping about the zero feathering axis a_1 are predicted to an accuracy of about 0.5° by the method of reference 2. In both cases the theoretical values are somewhat higher than the experimental values, the difference between the theoretical and experimental coning angles being the larger. This difference can also be seen in figure 16 in which the theoretical and experimental coefficients of the flapping about the zero feathering axis are plotted against the angle of attack of the zero feathering axis for $C_T = 0.00364$ and $\mu = 0.18$. It should be noted that the differences between the theoretical and experimental variations of the coefficients with angle of attack are within the accuracy of the measurements. The difference between the coning angles indicates that either the radial position of the blade thrust is inboard of the value calculated from the theory of reference 2 or the tip losses are greater than assumed.

The theoretical values of the lateral component of the equivalent flapping b_1 are found to be about 1.0° to 1.5° smaller than the values obtained in these tests. The theoretical and experimental variations of b_1 with μ and C_T, however, are in good agreement. It was shown in reference 5 that for the autogiro a similar difference exists between data and theoretical predictions based on a uniform inflow over the entire rotor disk and that the calculated value of b_1 is critically dependent upon the longitudinal variation of the induced velocity. In addition, it was shown in reference 5 that, if there is added to the originally assumed uniform induced velocity v an additional velocity v_1 of the form

$$v_1 = Kv \frac{r}{R} \cos \psi \tag{1}$$

where K is the ratio of v_1 to v when $\psi = 0^\circ$ and $r = R$, so that the total induced velocity becomes

$$v' = v + v_1 \tag{2}$$

then the change in b_1 can be written as

$$\Delta b_1 = \frac{KB^2C_T}{2\left(B^2 + \frac{1}{2}\mu^2\right)\left(\mu^2 + \lambda^2\right)^{1/2}} \tag{3}$$

In reference 5, however, no means was given for calculating the factor K. In reference 3 the induced velocity is calculated for a rotor by assuming a simplified vortex system in the wake of the rotor. An approximation to the exact solution was taken in reference 3 to be of the form of equations (1) and (2).

By use of the values of K determined in this manner, the value of Δb_1 was found. The values of b_1 obtained from this nonuniform inflow theory are plotted in figures 13 and 15; the agreement with the data is closer than that obtained with the uniform-inflow-theory calculations. The calculated change in b_1, however, is of sufficient magnitude to account for slightly less than half the difference between the data and the constant inflow calculations, which suggests that the longitudinal variation of the inflow through the rotor tested was larger than that calculated by either method.

A study, based on the methods and results of references 6 and 7, was made to estimate the effects of the longitudinal variation of jet-boundary corrections on the blade motion of the rotor. This analysis indicated that while some longitudinal variation of the induced velocities due to the jet existed, the magnitude of this variation was too small to account for any significant part of the differences between the experimental values of b_1 and the values calculated by using the linear nonuniform inflow obtained from reference 3. The difference between the data and the nonuniform theory is probably due to the simplifying assumptions made in reference 3.

CONCLUSIONS

The flapping and feathering motions of the 0.75-radius station have been obtained experimentally for the PV-2 helicopter rotor over a range of forward-flight conditions with the rotor trimmed about a representative center-of-gravity location. The results have been presented in a convenient set of charts from which the blade motions of such a rotor can be obtained. These results indicate the following:

1. The magnitude of the measured flapping motion is small, less than 1°, for a rotor that is trimmed about a point on the shaft and below the rotor head. The second harmonics of the flapping motion are very small, less than 0.25°, which is in accord with the theoretical predictions.

2. Both the lateral and longitudinal components of the feathering required to trim the rotor increase in magnitude with tip-speed ratio and thrust coefficient.

3. Relatively large errors in determining useful drag-lift ratio $(D/L)_u$ resulted in only secondary errors in the determination of the blade-motion coefficients within the range of these tests ($(D/L)_u$ between 0.04 and 0.2).

4. The theory based on the assumption of uniform inflow velocity across the rotor disk predicts the coning angle a_0 and the longitudinal component of the equivalent flapping a_1 to an accuracy of about 0.5°.

5. Theoretical calculations, based on the assumption of uniform inflow, are found to be approximately 1.0° to 1.5° smaller than the experimental values of the lateral component of equivalent flapping b_1. The theoretical and experimental variations of b_1 with tip-speed ratio and thrust coefficient, however, are in good agreement. The use of an inflow that increases linearly from the front to the rear of the rotor accounts for approximately one-half the difference between the data and the values obtained by the uniform-inflow theory.

Langley Memorial Aeronautical Laboratory
National Advisory Committee for Aeronautics
Langley Field, Va., September 2, 1947

REFERENCES

1. Migotsky, Eugene: Full-Scale-Tunnel Performance Tests of the PV-2 Helicopter Rotor. NACA MR No. L5C29a, 1945.

2. Bailey, F. J., Jr.: A Simplified Theoretical Method of Determining the Characteristics of a Lifting Rotor in Forward Flight. NACA Rep. No. 716, 1941.

3. Coleman, Robert P., Feingold, Arnold M., and Stempin, Carl W.: Evaluation of the Induced-Velocity Field of an Idealized Helicopter Rotor. NACA ARR No. L5E10, 1945.

4. Lock, C. N. H.: Further Development of Autogyro Theory. Parts I and II. R. & M. No. 1127, British A.R.C., 1928.

5. Wheatley, John B.: An Aerodynamic Analysis of the Autogiro Rotor with a Comparison between Calculated and Experimental Results. NACA Rep. No. 487, 1934.

6. Silverstein, Abe, and White, James A.: Wind-Tunnel Interference with Particular Reference to Off-Center Positions of the Wing and to the Downwash at the Tail. NACA Rep. No. 547, 1935.

7. Silverstein, Abe, and Katzoff, S.: Experimental Investigation of Wind-Tunnel Interference on the Downwash behind an Airfoil. NACA Rep. No. 609, 1937.

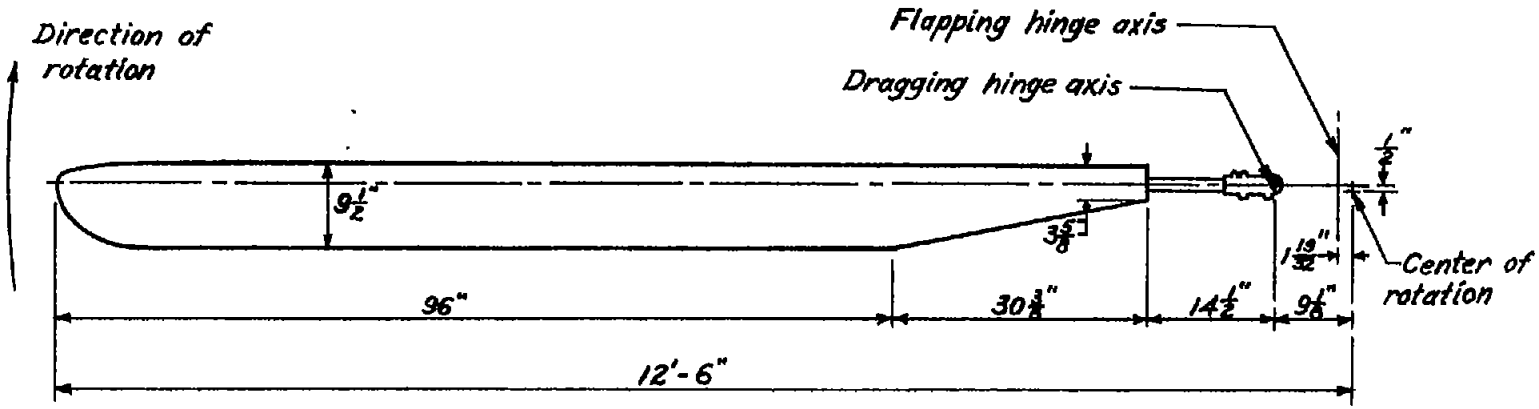

Weight, lb	16.0
Weight moment about flapping hinge, M_w, lb-ft	95.8
Mass moment of inertia about flapping hinge, I_1, slug-ft^2	25.14
Mass constant, γ	10.16

Figure 1.- Physical characteristics of PV-2 helicopter rotor blade.

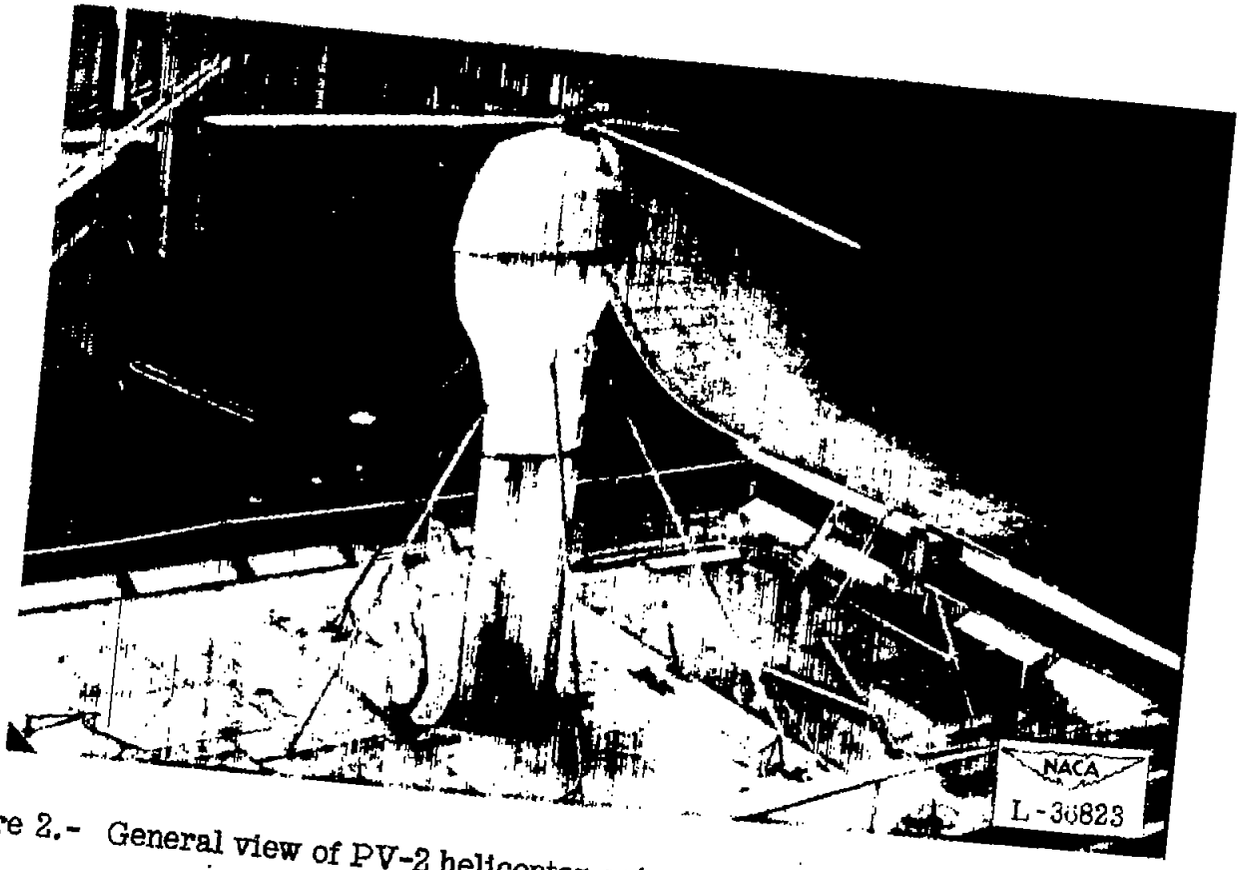

Figure 2.- General view of PV-2 helicopter rotor mounted in Langley full-scale tunnel.

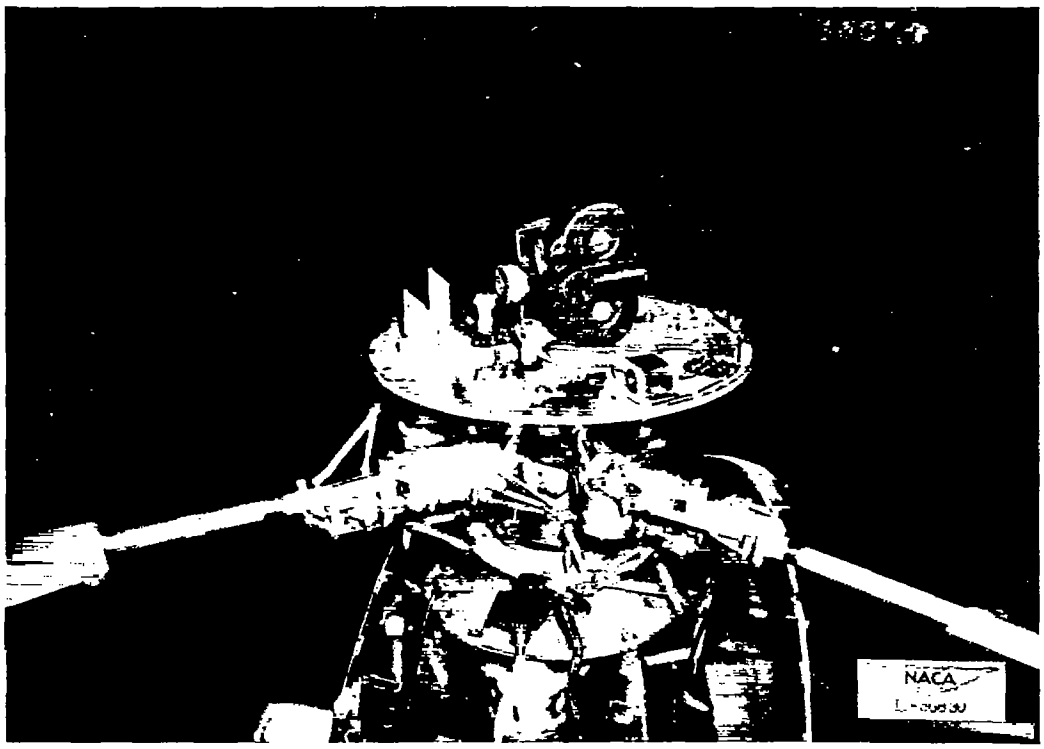

Figure 3.- Camera mounted on rotor hub.

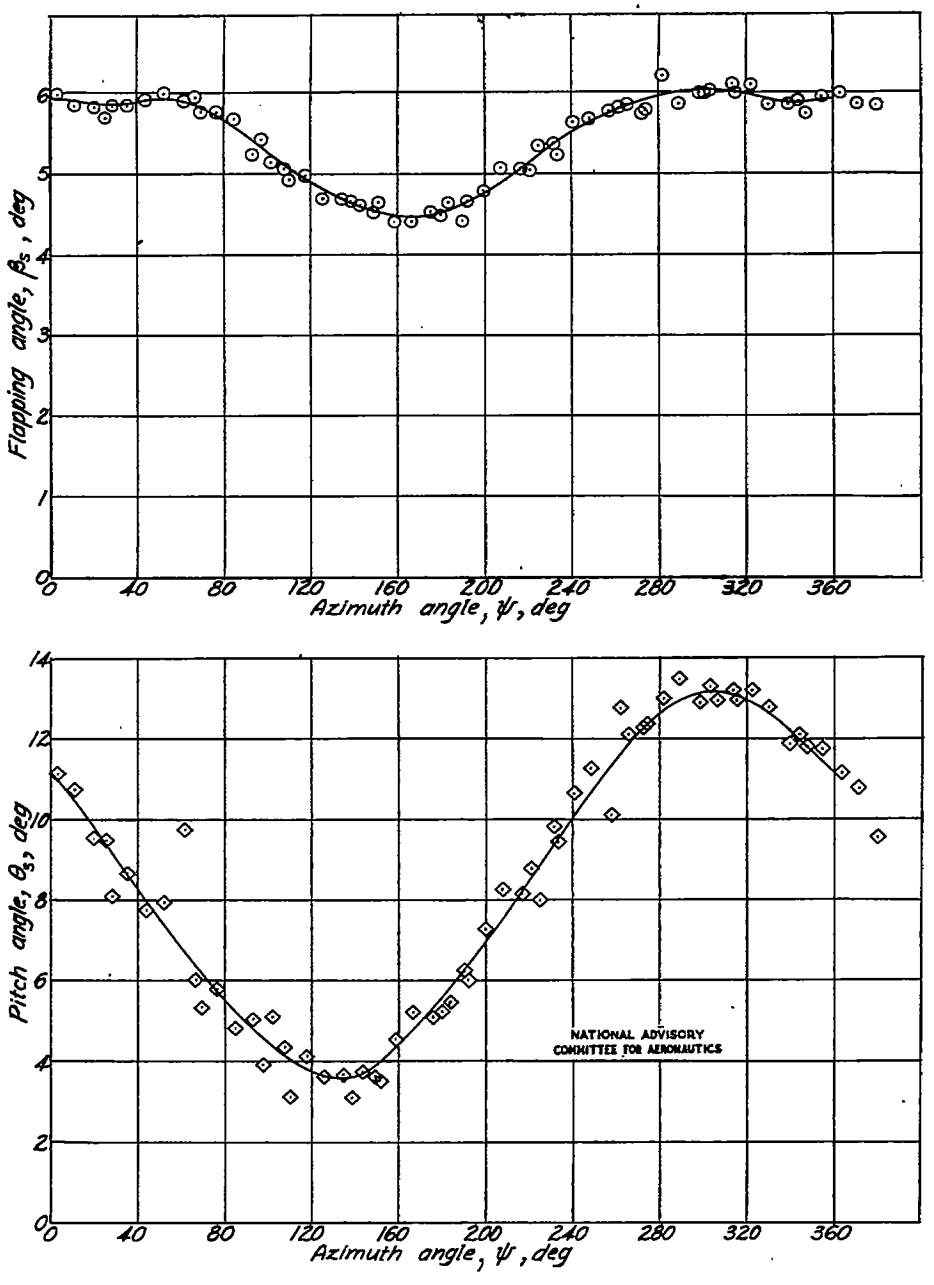

Figure 4.- Sample variation of measured flapping and pitch angles with azimuth angle for the 0.75-radius station. PV-2 helicopter rotor; μ = 0.187; α_{s_T} = -5.5°; A_{O_s} = 8.4°; rotor speed, approximately 270 rpm.

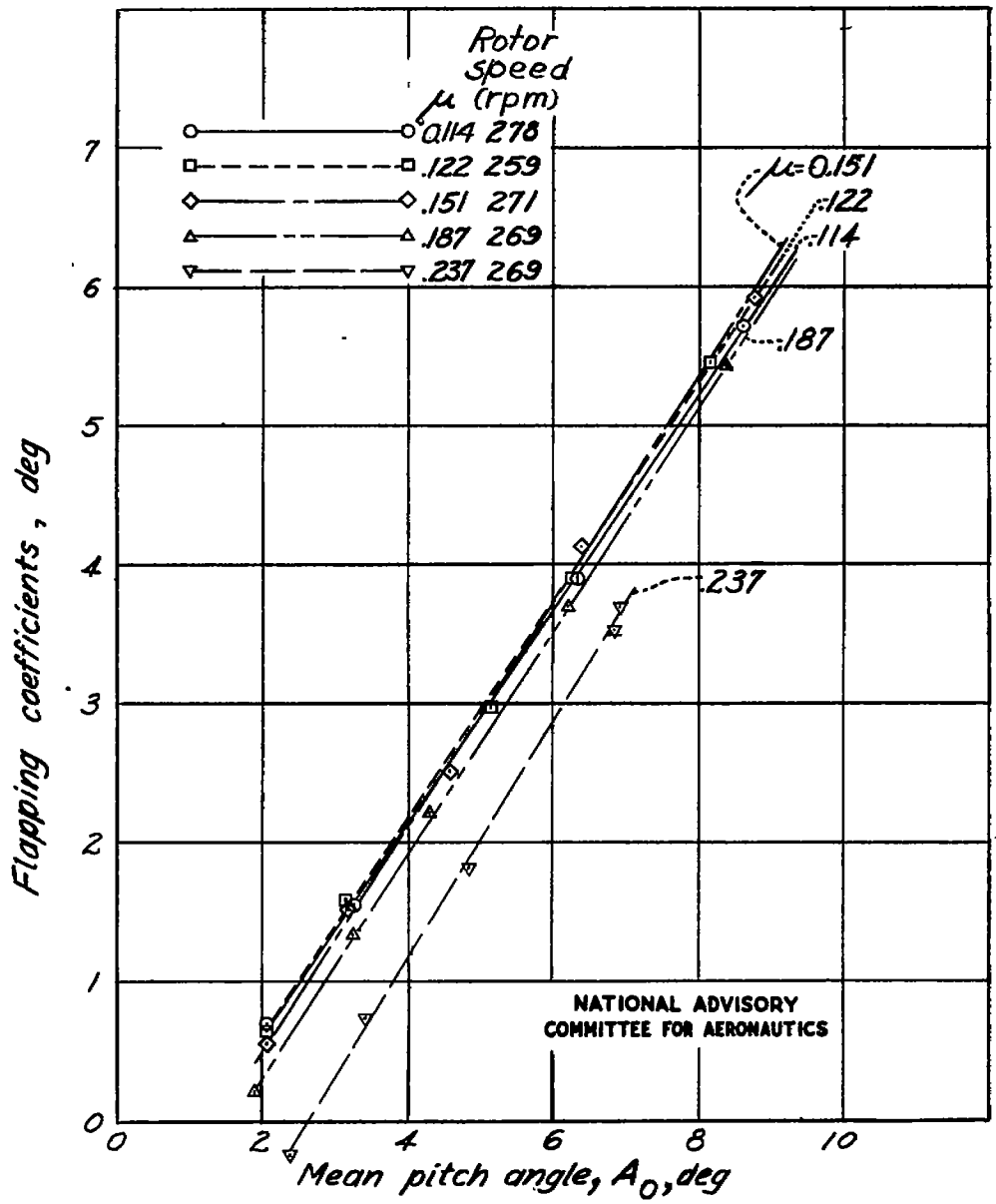

(a) Coning angle, a_{0_s}.

Figure 5.- Variation of measured flapping coefficients with mean pitch angle for several values of tip-speed ratio. PV-2 helicopter rotor; $\alpha_{s_T} = -5.5^{\circ}$.

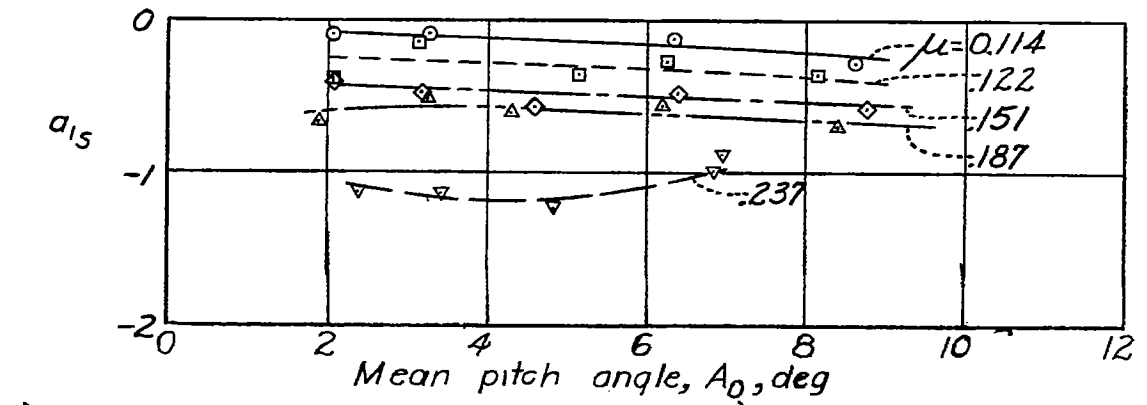

(b) First-harmonic cosine coefficient, a_{1_s}.

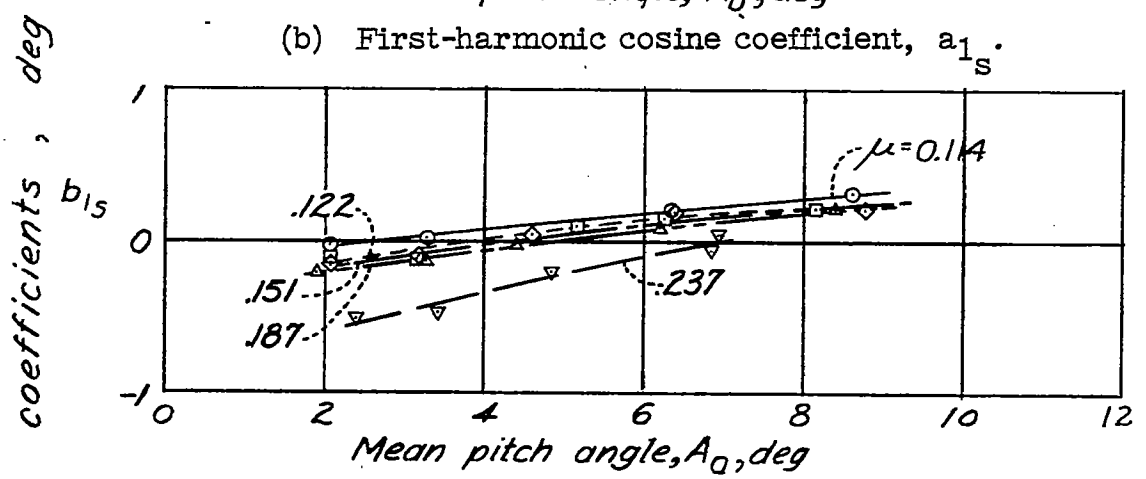

(c) First-harmonic sine coefficient, b_{1_s}.

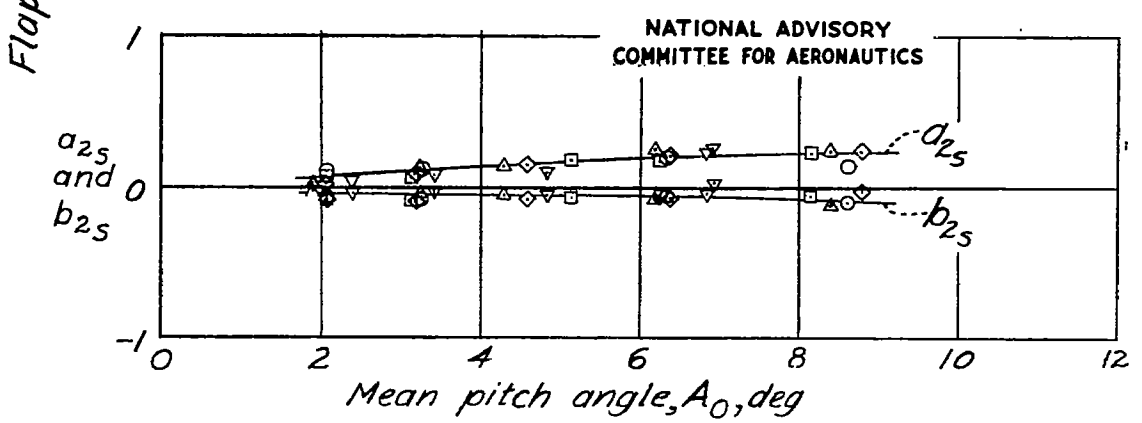

(d) Second-harmonic cosine and sine coefficients, a_{2_s} and b_{2_s}.

Figure 5.- Concluded.

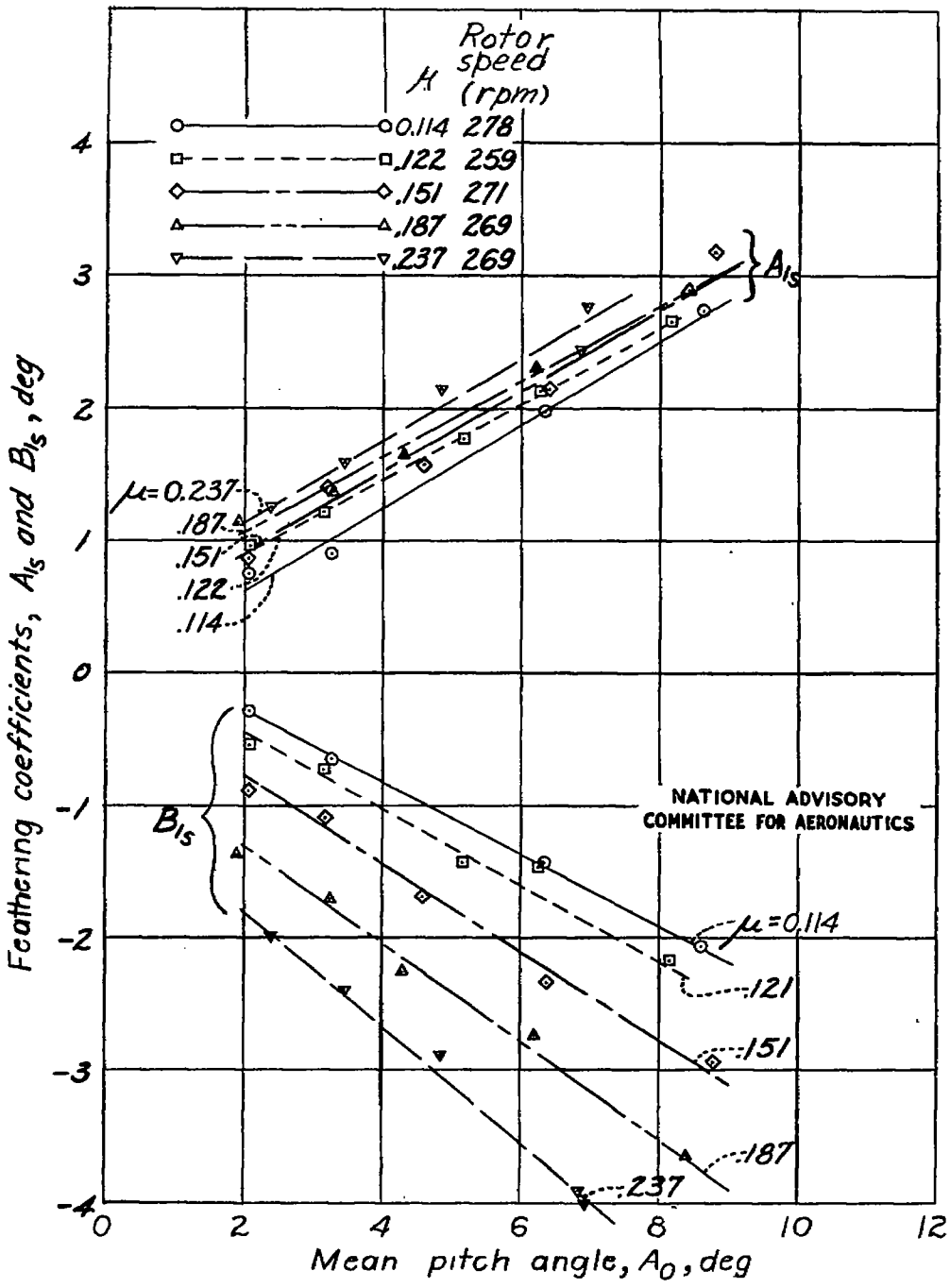

Figure 6.- Variation of measured feathering coefficients with mean pitch angle for several values of tip-speed ratio. PV-2 helicopter rotor; $\alpha_{s_T} = -5.5^{\circ}$.

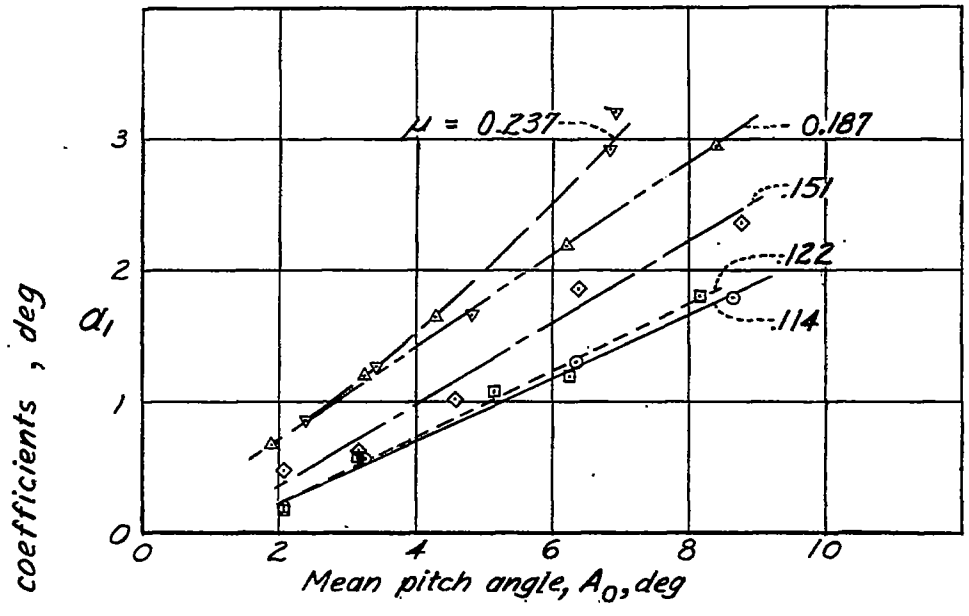

(a) First-harmonic cosine coefficient, a_1.

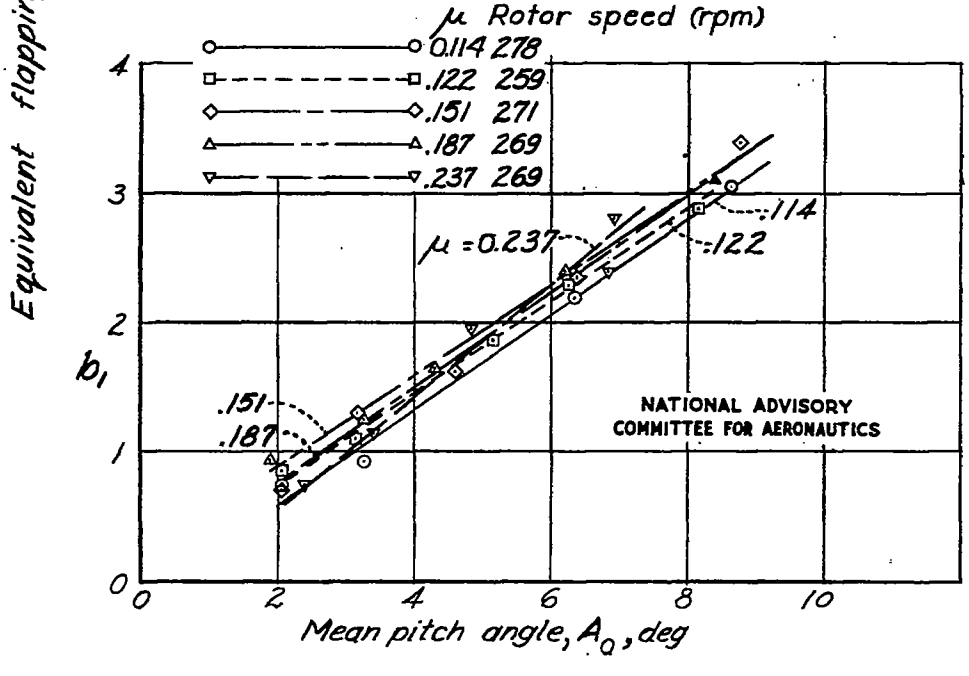

(b) First-harmonic sine coefficient, b_1.

Figure 7.- Variation of equivalent flapping coefficients with mean pitch angle for several values of tip-speed ratio. PV-2 helicopter rotor; $\alpha_{s_T} = -5.5^{\circ}$.

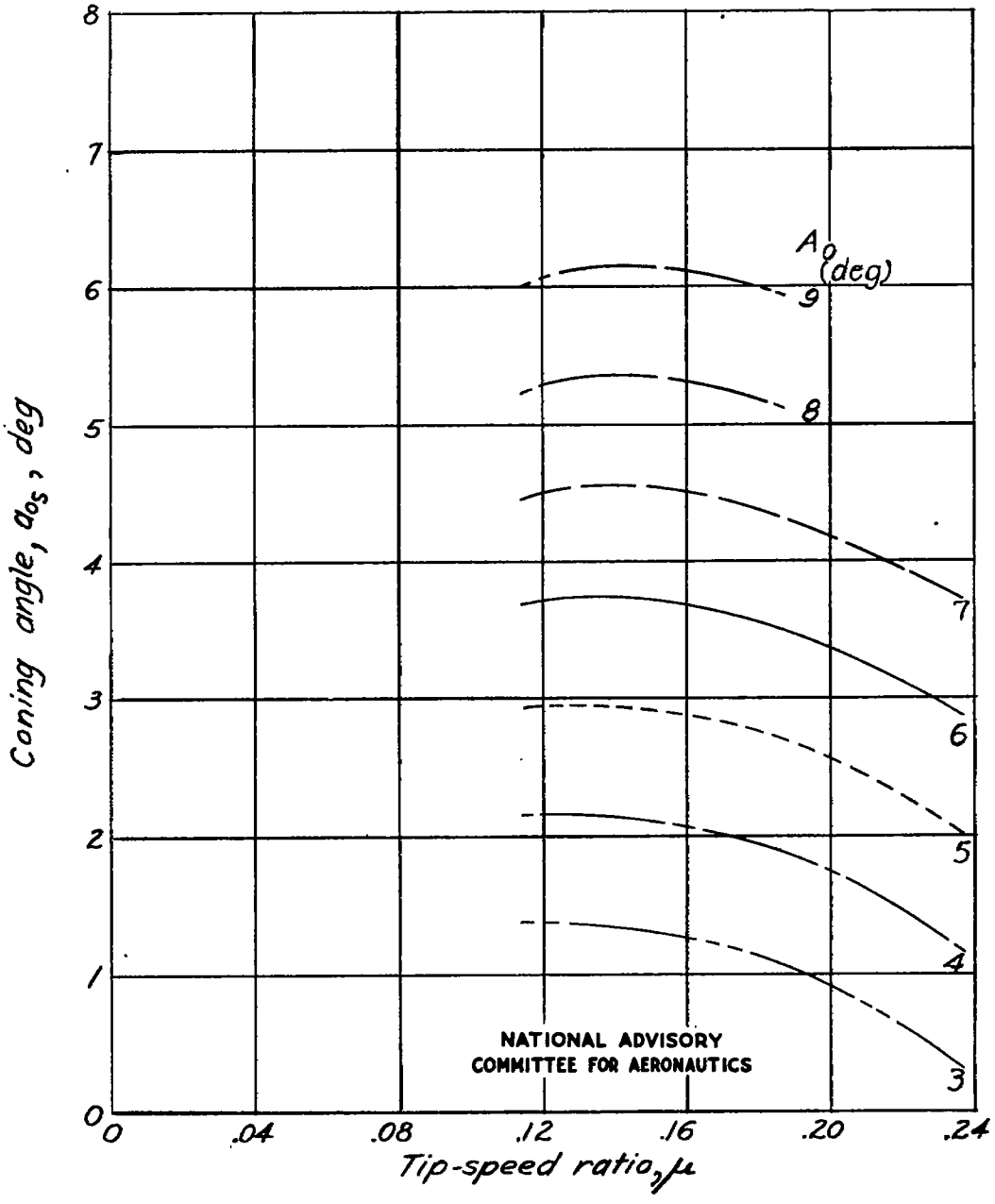

(a) Coning angle, a_{O_S}.

Figure 8.- Variation of blade-motion coefficients with tip-speed ratio for different values of mean pitch angle. PV-2 helicopter rotor; rotor speed, approximately 270 rmp; $\alpha_{s_T} = -5.5^{\circ}$.

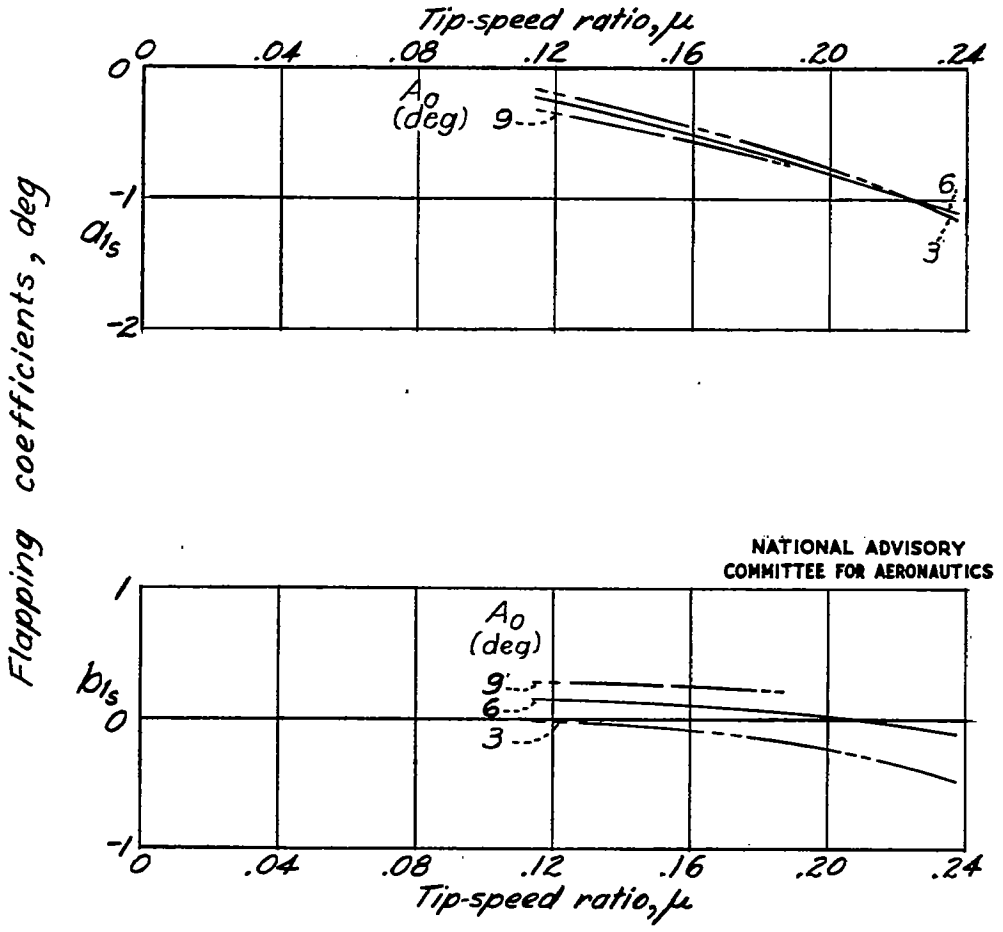

(b) Measured flapping coefficients, a_{1_s} and b_{1_s}.

Figure 8.- Continued.

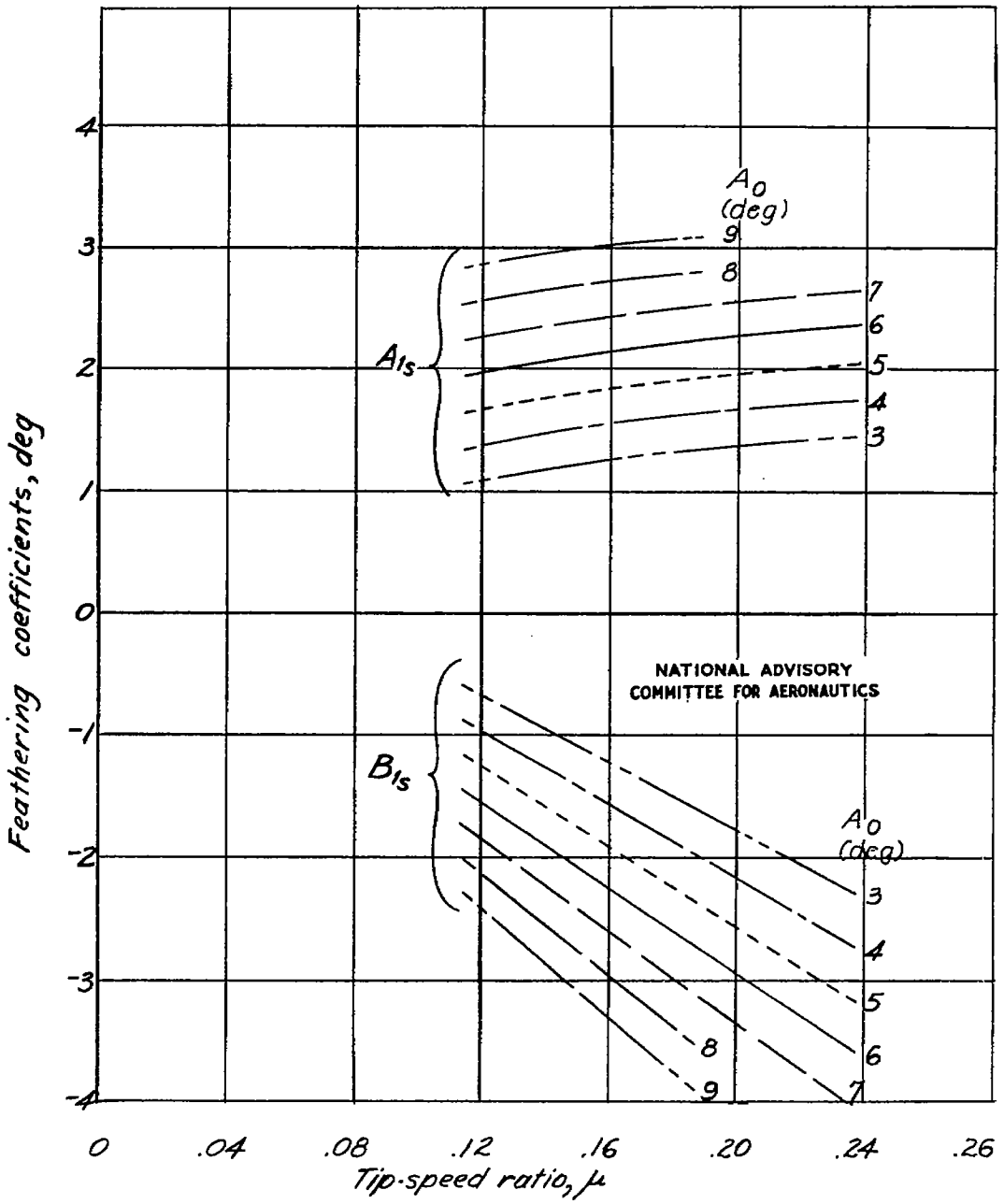

(c) Measured feathering coefficients, A_{1_s} and B_{1_s}.

Figure 8.- Continued.

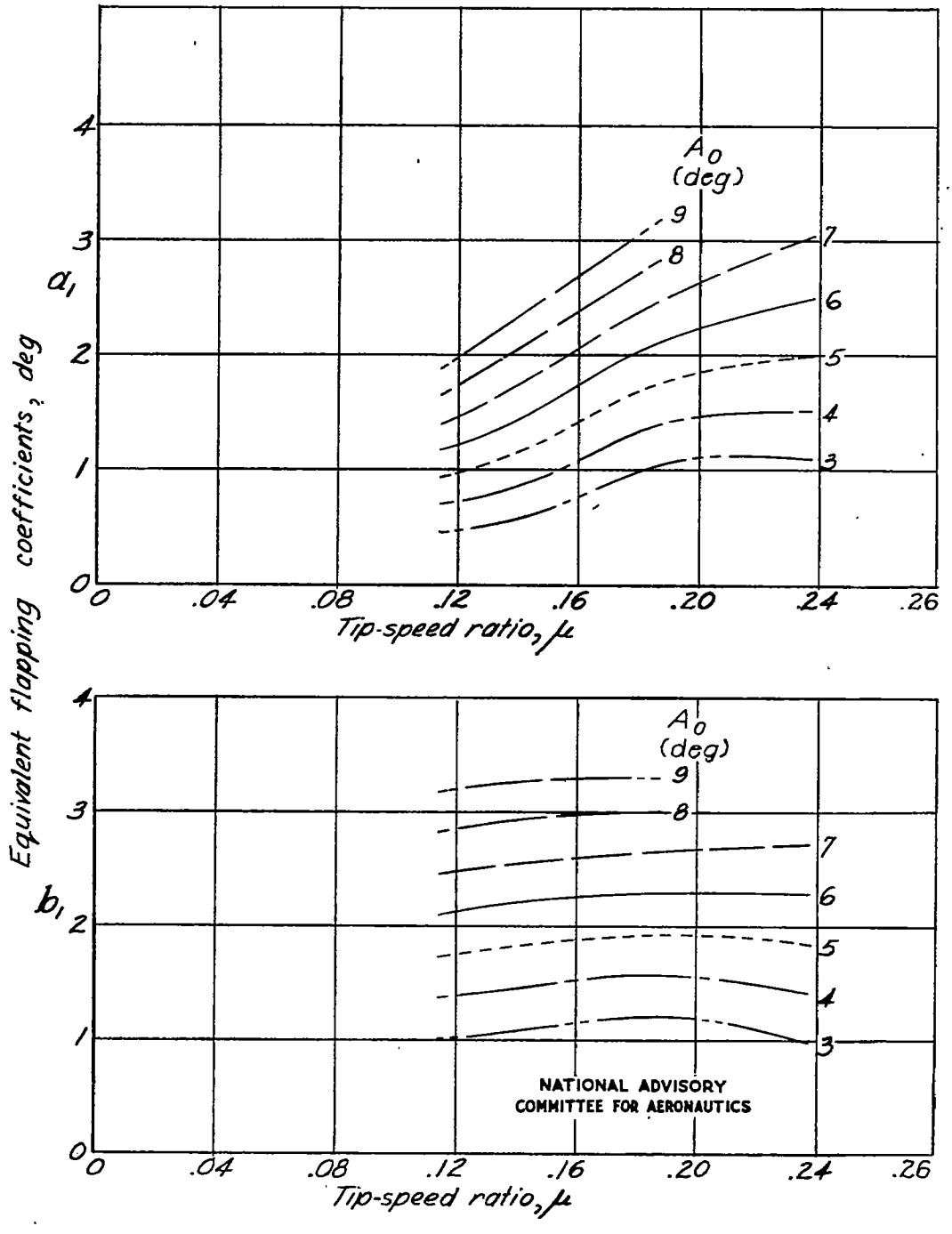

(d) Equivalent flapping coefficients, a_1 and b_1.

Figure 8.- Concluded.

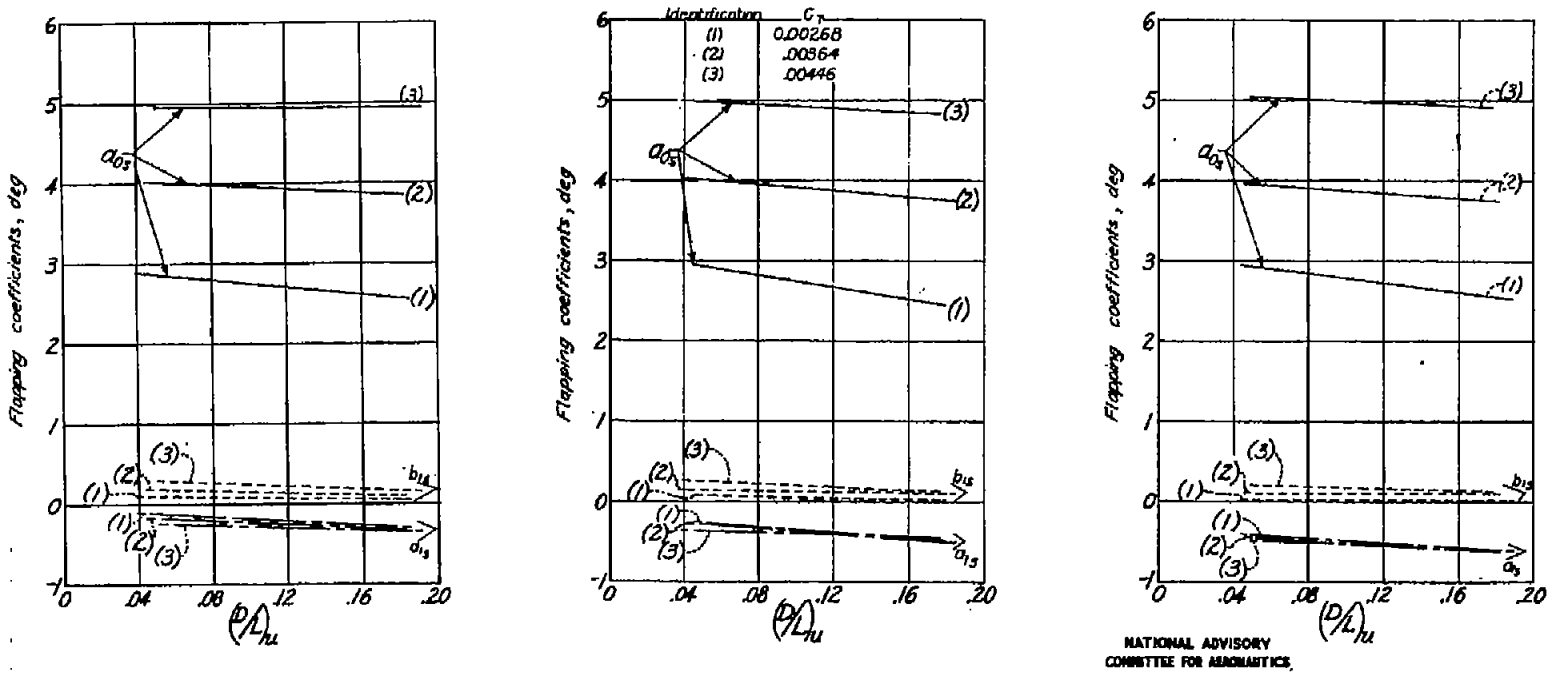

(a) $\mu = 0.12$.

(b) $\mu = 0.14$.

(c) $\mu = 0.16$.

Figure 9.- Measured flapping coefficients as functions of $(D/L)_u$. PV-2 helicopter rotor.

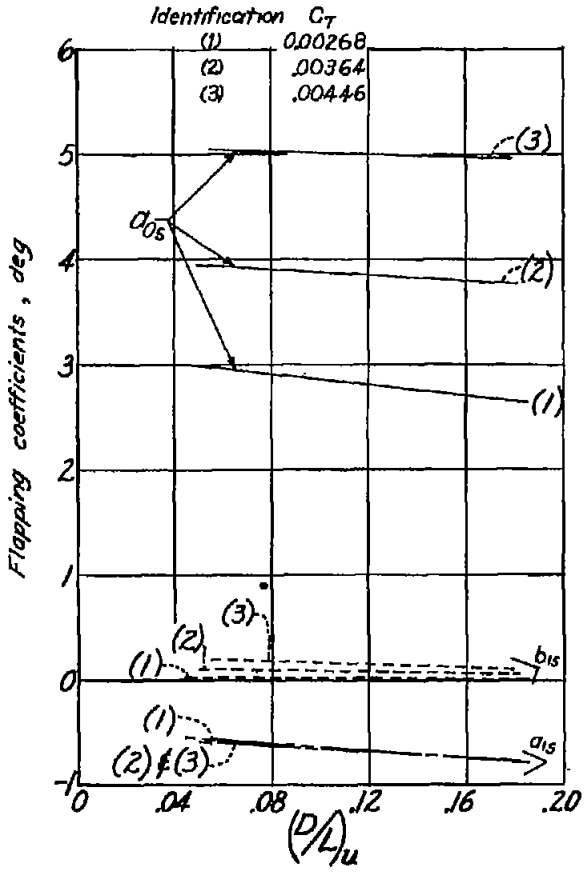

(d) $\mu = 0.18$.

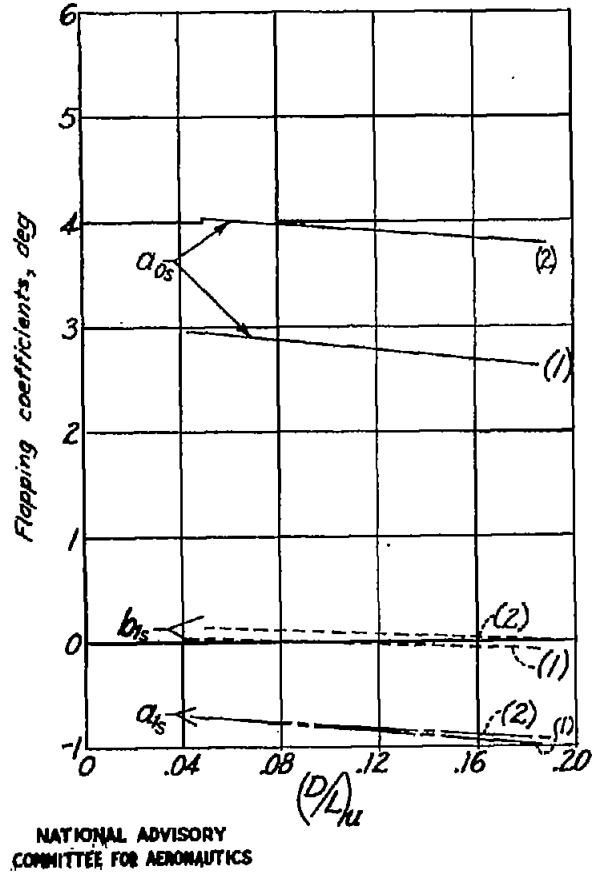

(e) $\mu = 0.20$.

Figure 9.- Concluded.

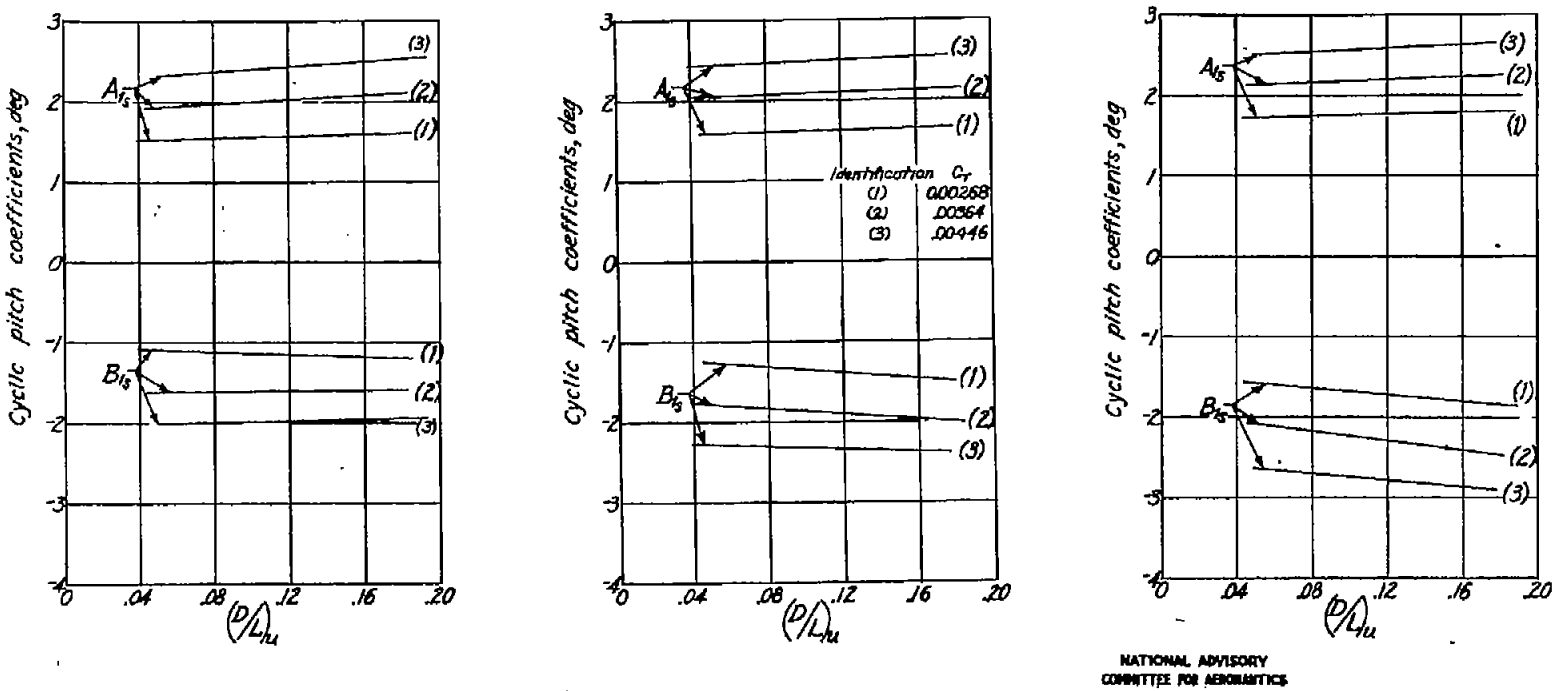

(a) μ = 0.12. (b) μ = 0.14. (c) μ = 0.16.

Figure 10.- Measured feathering coefficients as function of $(D/L)_u$. PV-2 helicopter rotor.

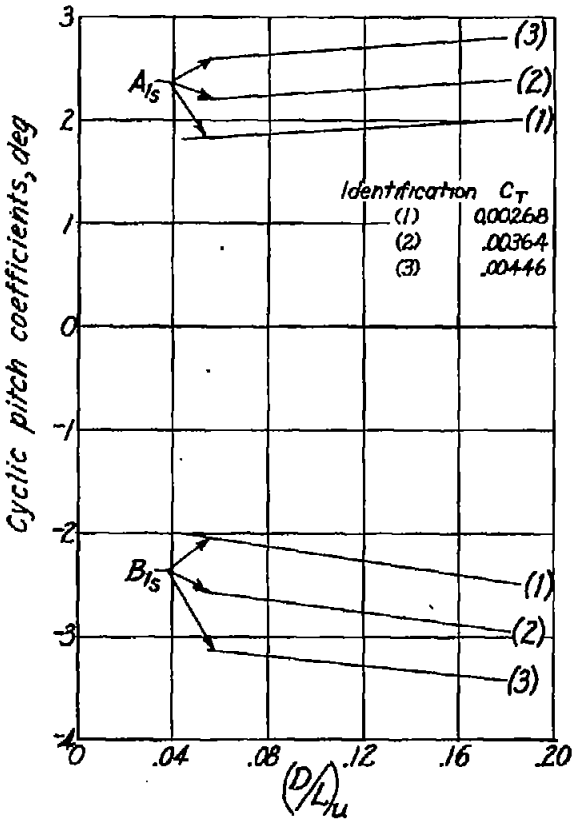

(d) $\mu = 0.18$.

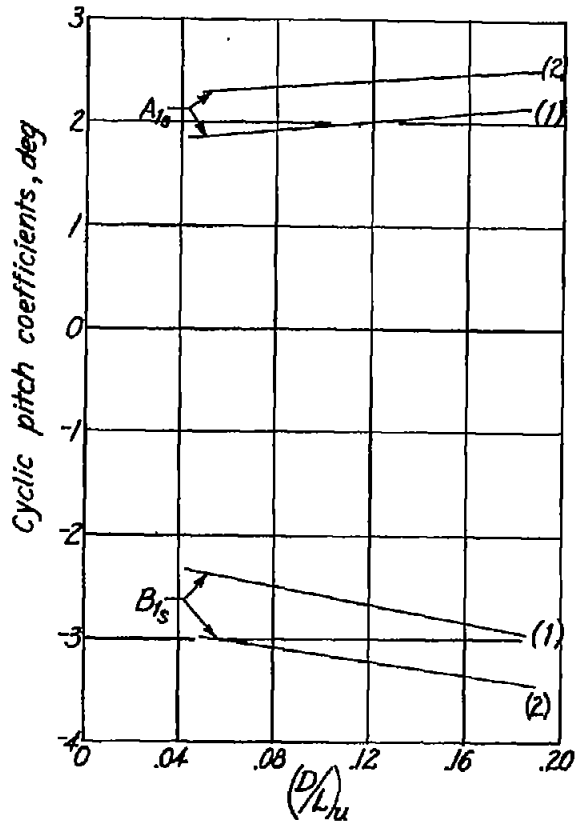

NATIONAL ADVISORY
COMMITTEE FOR AERONAUTICS

(e) $\mu = 0.20$.

Figure 10.- Concluded.

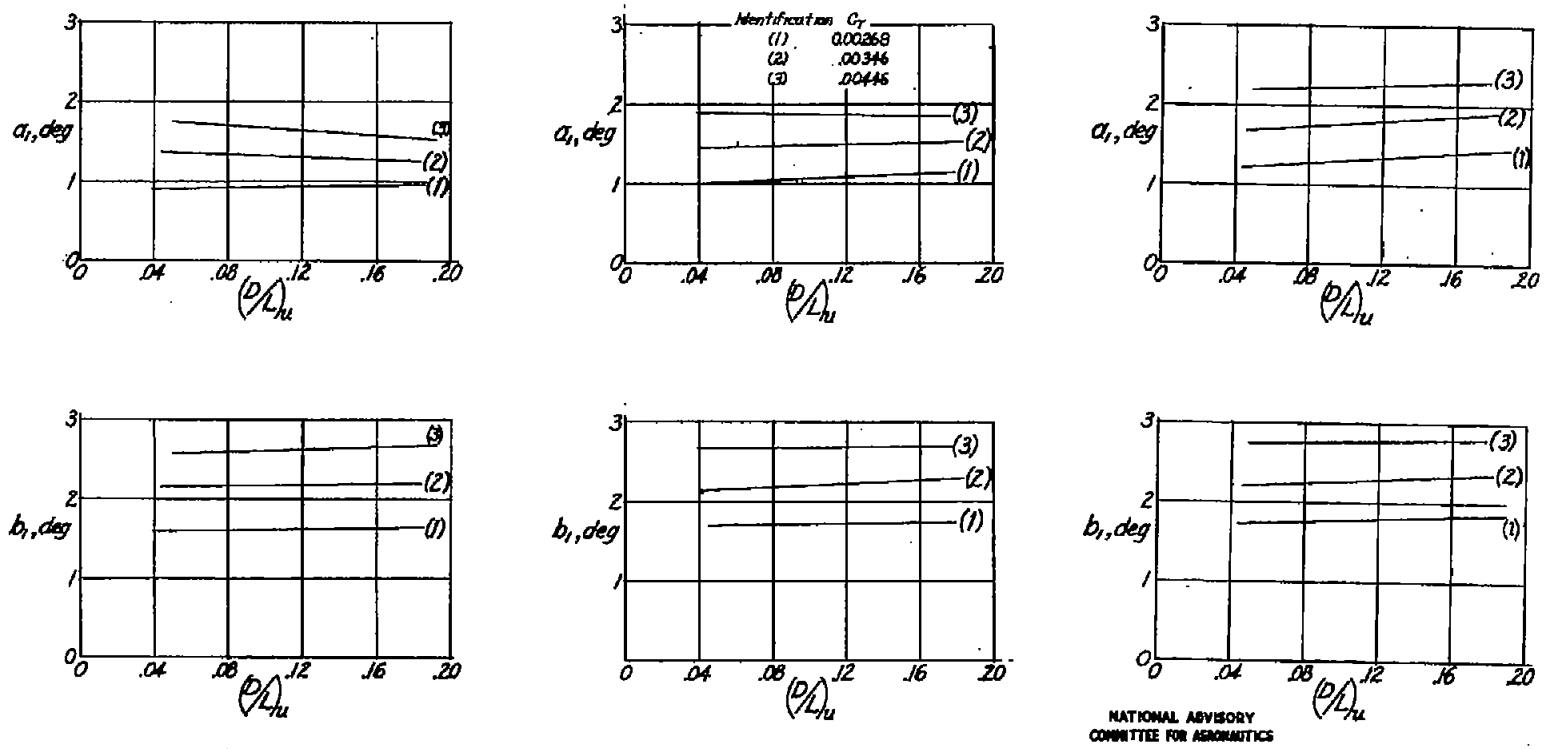

(a) $\mu = 0.12$. (b) $\mu = 0.14$. (c) $\mu = 0.16$.

Figure 11.- Equivalent flapping coefficients as function of $(D/L)_u$. PV-2 helicopter rotor.

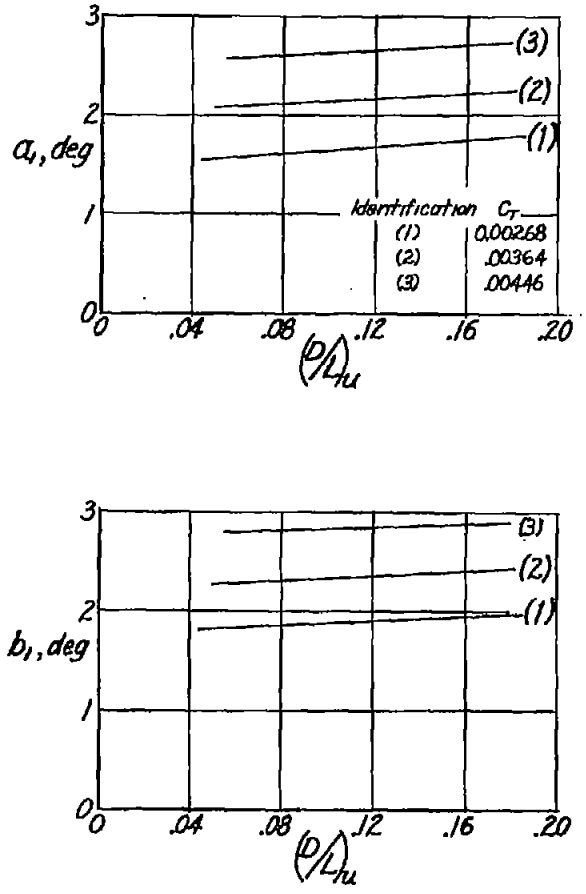

(d) $\mu = 0.18$.

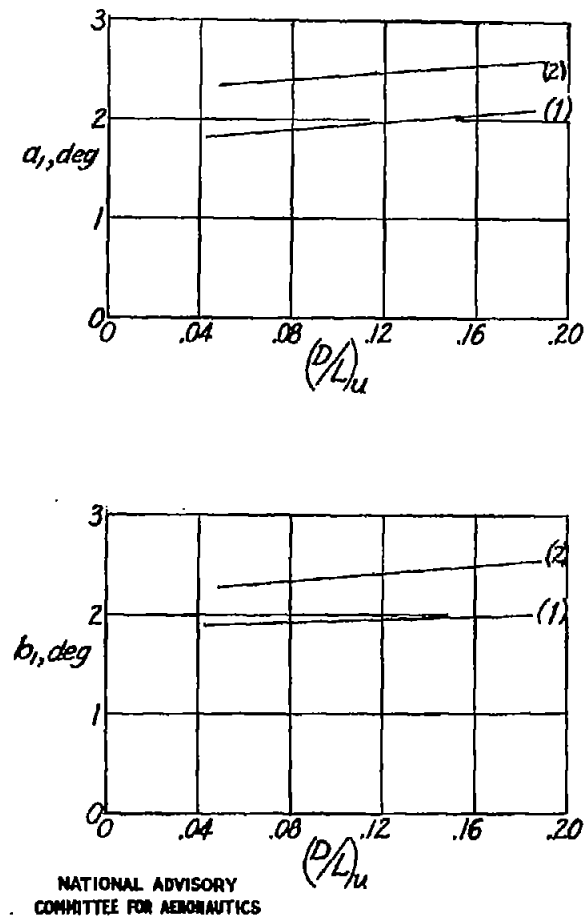

(e) $\mu = 0.20$.

Figure 11.- Concluded.

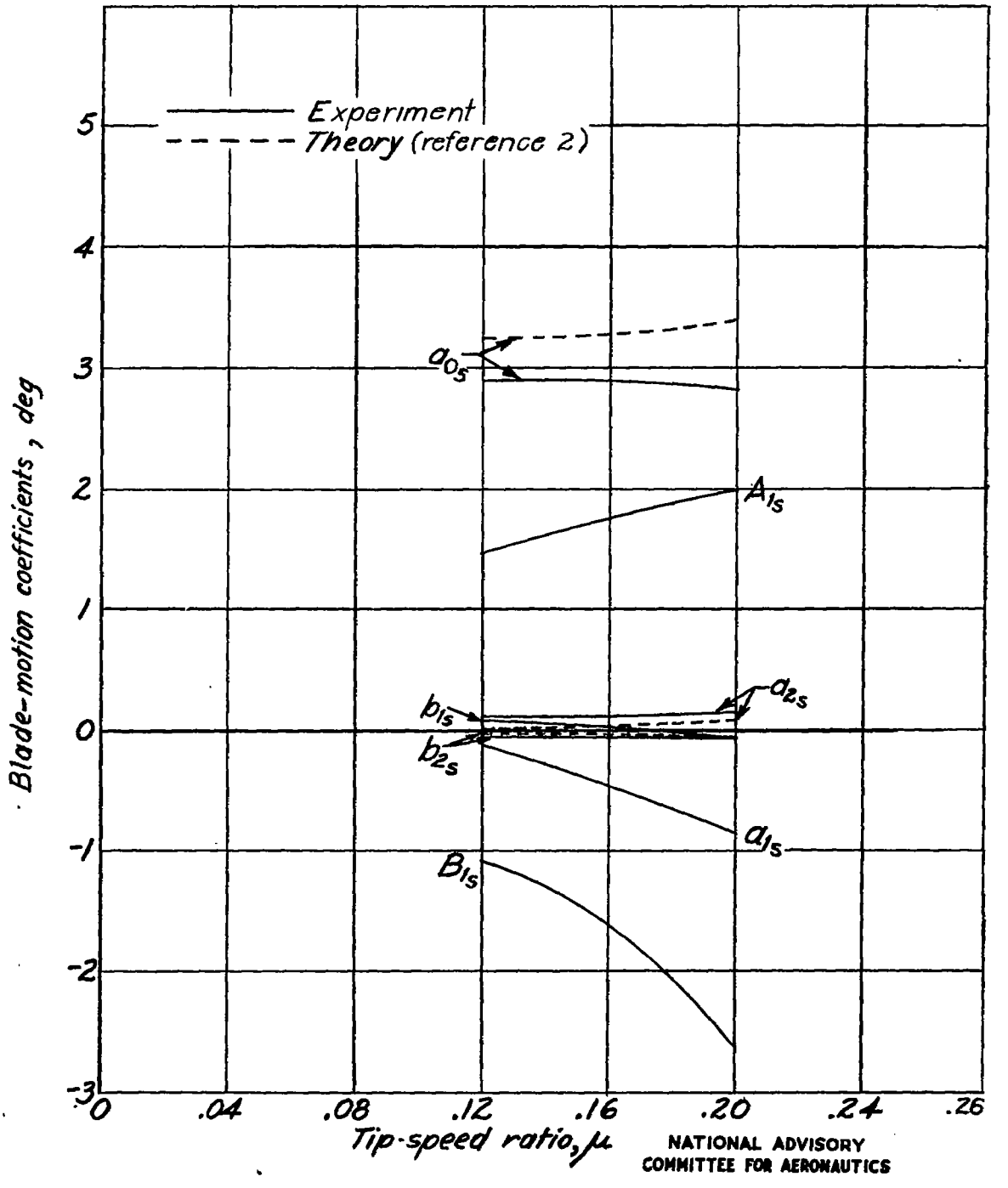

(a) $C_T = 0.00268$.

Figure 12.- Blade-motion coefficients as functions of tip-speed ratio. PV-2 helicopter rotor; f = 7 square feet.

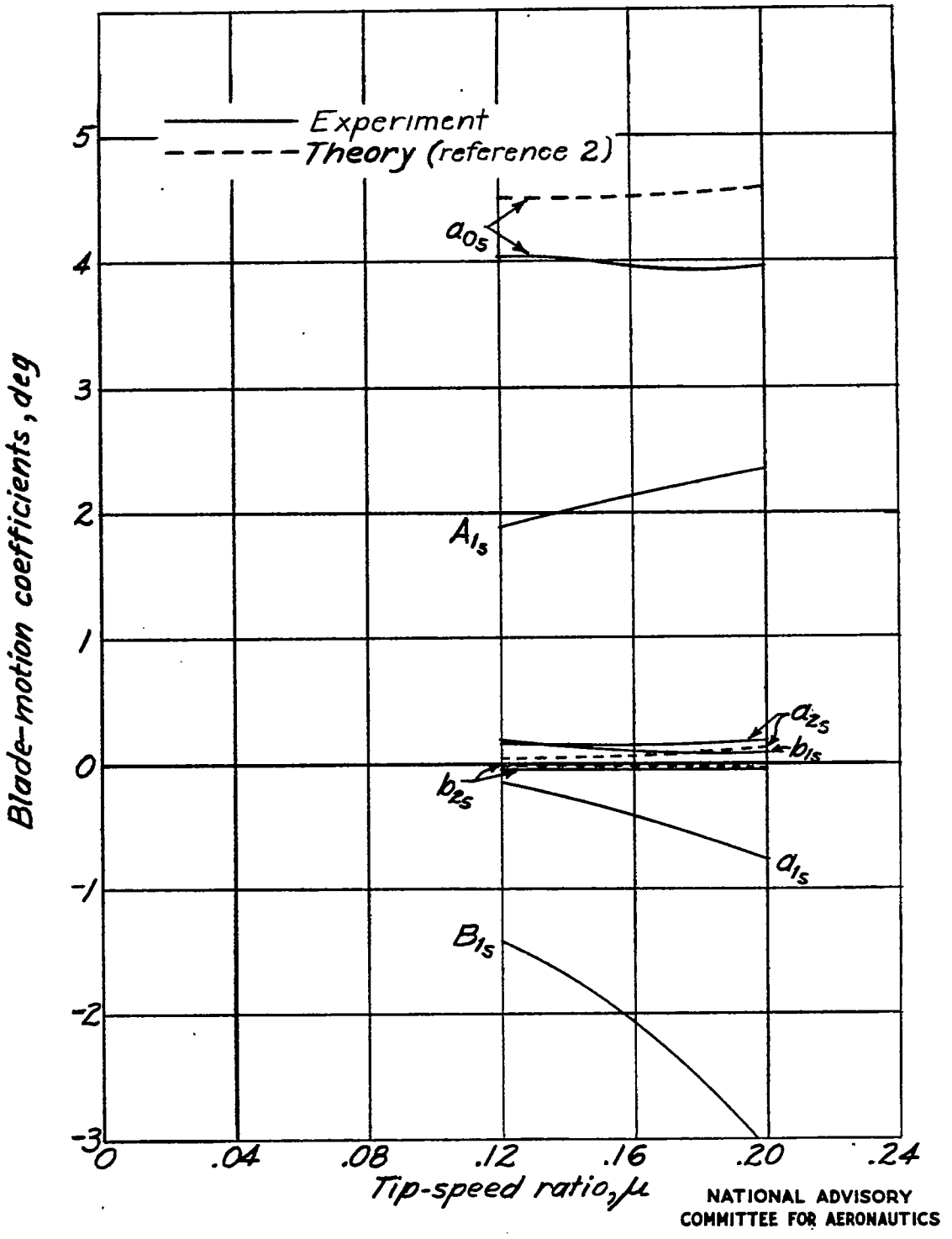

(b) $C_T = 0.00364$.

Figure 12.- Continued.

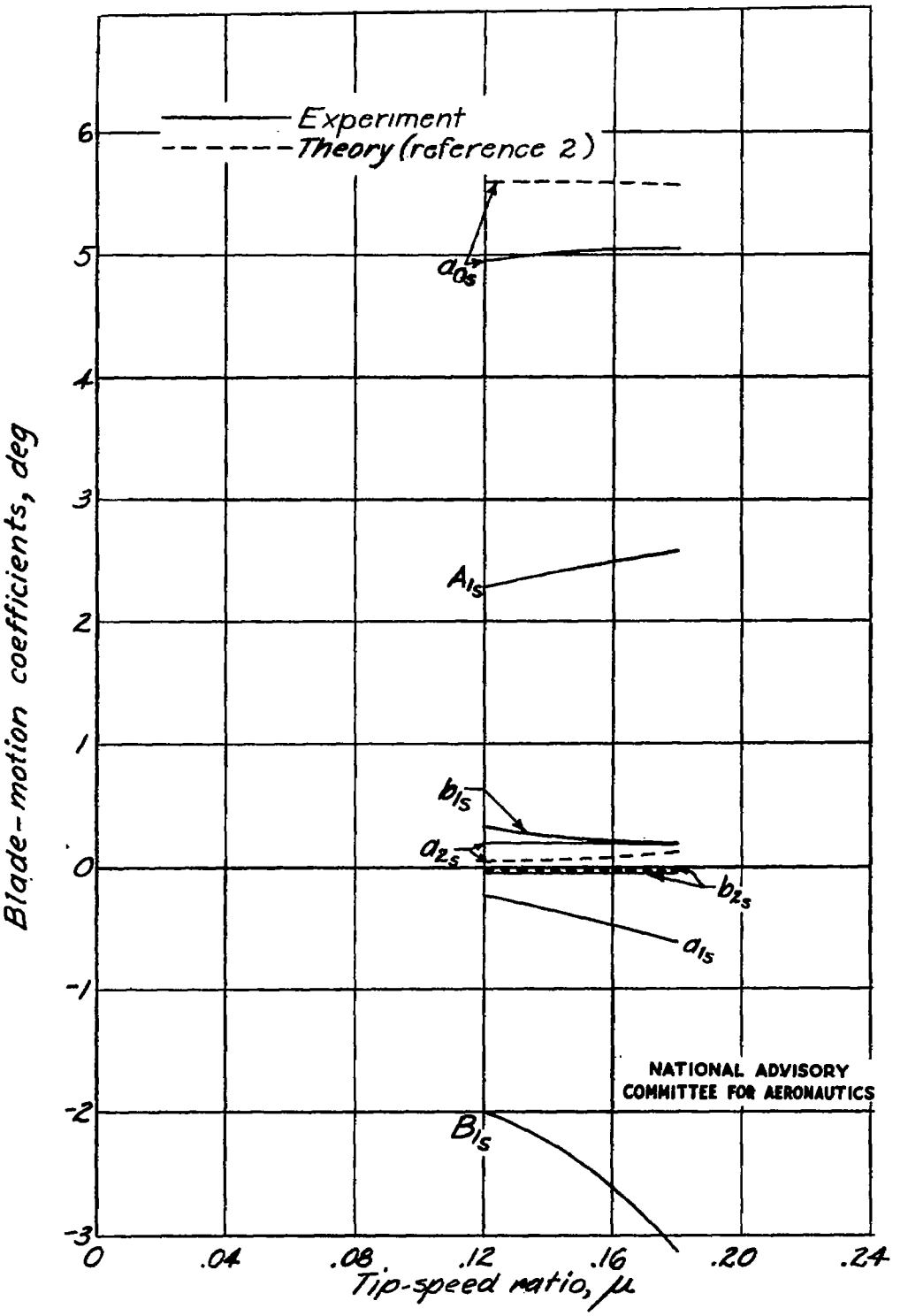

(c) $C_T = 0.00446$.

Figure 12.- Concluded.

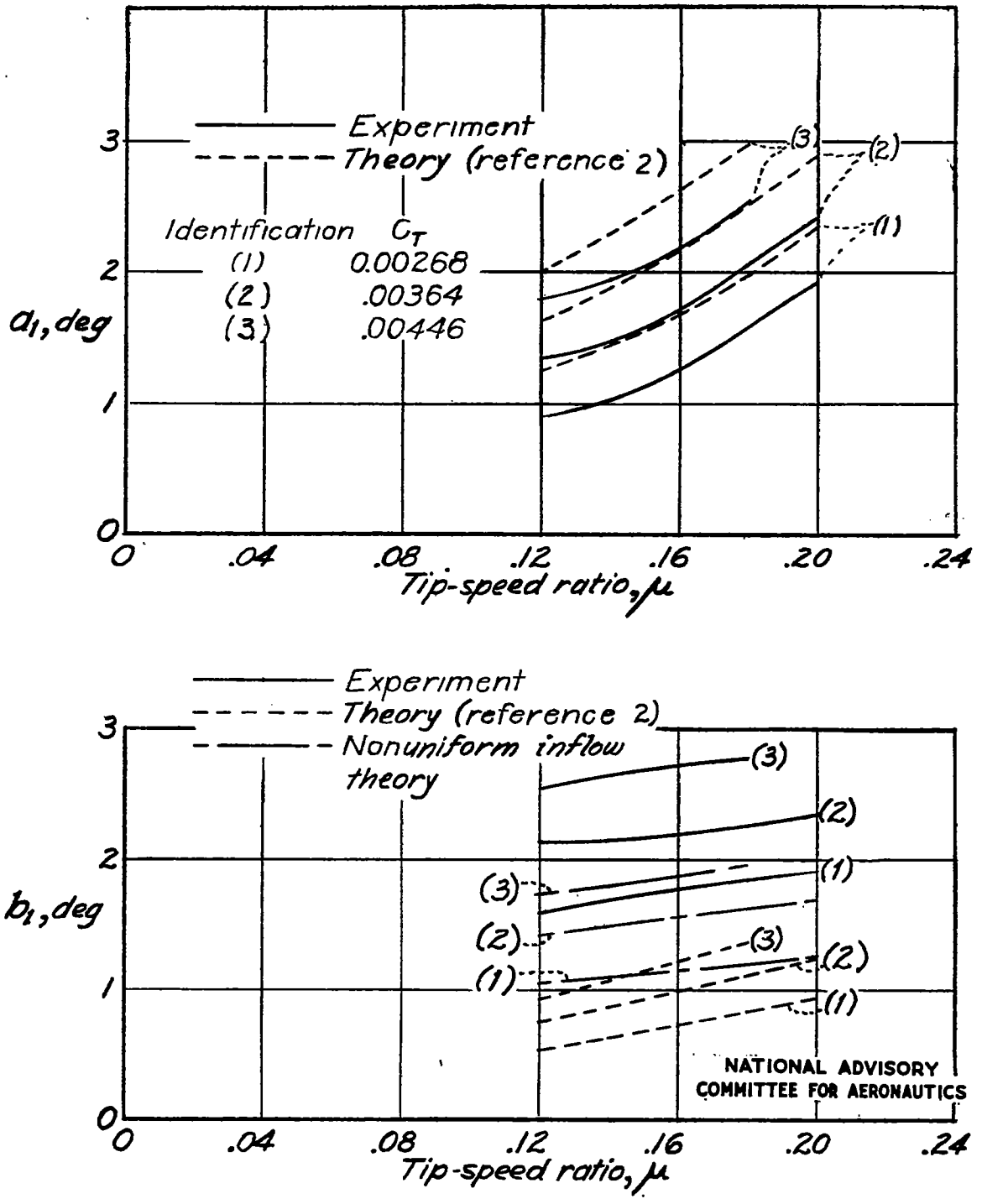

Figure 13.- Equivalent flapping coefficients as functions of tip-speed ratio. PV-2 helicopter rotor; f = 7 square feet.

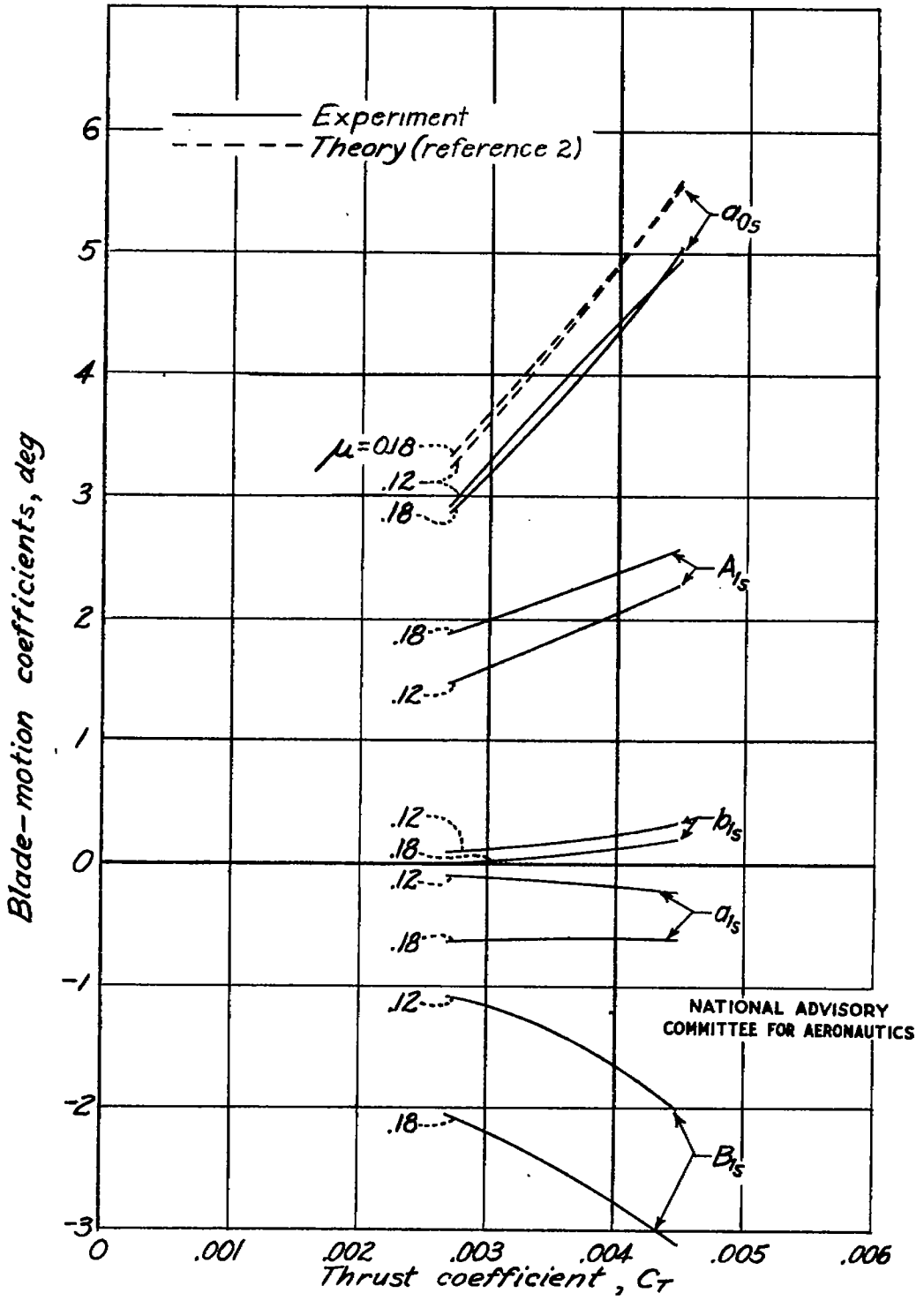

Figure 14.- Variation of blade-motion coefficients with thrust coefficient. PV-2 helicopter rotor; f = 7 square feet.

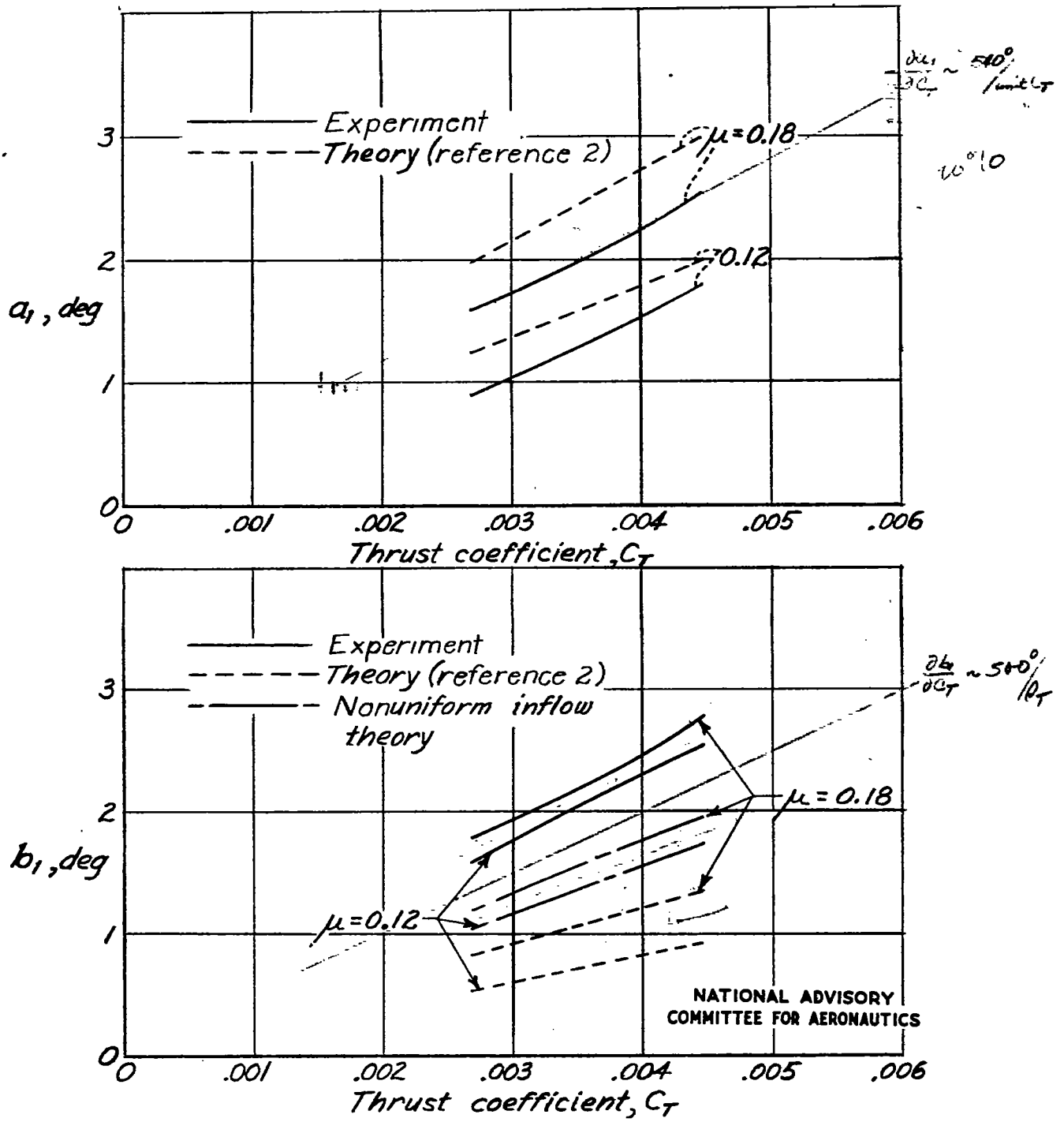

Figure 15.- Variation of equivalent flapping coefficients with thrust coefficient. PV-2 helicopter rotor; f = 7 square feet.

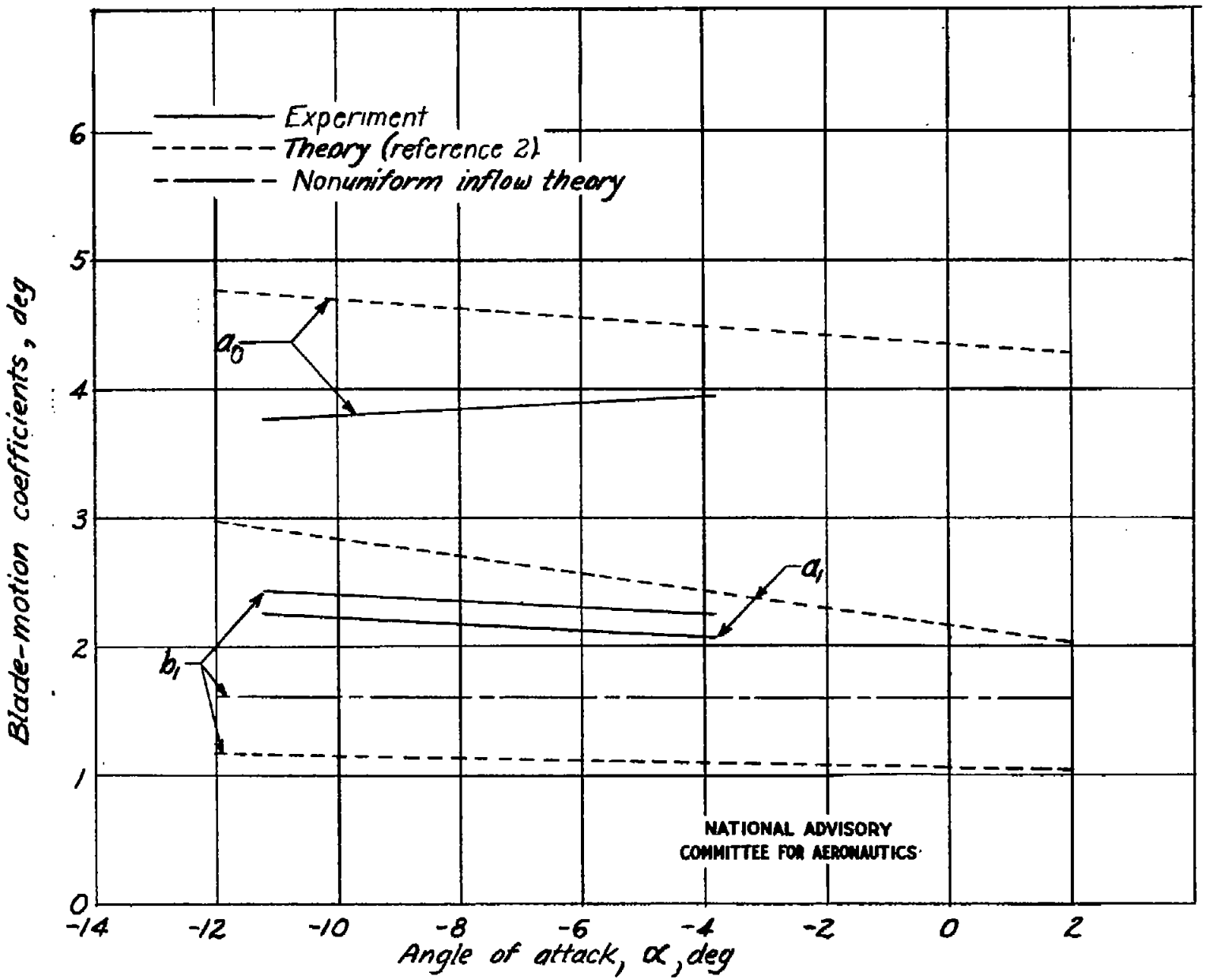

Figure 16.- Equivalent flapping coefficients as functions of rotor angle of attack. PV-2 helicopter rotor; $C_T = 0.00364$; $\mu = 0.18$.